Applied Energy xxx (2017) xxx–xxx

Contents lists available at ScienceDirect

Applied Energy

journal homepage: www.elsevier.com/locate/apenergy

Optimization of unit commitment and economic dispatch in microgrids based on genetic algorithm and mixed integer linear programming

Mohsen Nemati [a,*], Martin Braun [b], Stefan Tenbohlen [c]

[a] Siemens AG, Humboldt Street 59, 90443 Nuremberg, Germany
[b] Fraunhofer IWES, University of Kassel, Kassel, Germany
[c] University of Stuttgart-IEH, Stuttgart, Germany

HIGHLIGHTS

- Day-ahead dispatching of the renewable energy resources inside a microgrid.
- Genetic algorithm based optimizer for solving unit commitment and economic dispatch.
- Aging model of the Li-Ion battery based on an event-driven method.
- Mixed integer linear programming for optimal power flow of microgrids.

ARTICLE INFO

Article history:
Received 31 March 2017
Received in revised form 6 June 2017
Accepted 10 July 2017
Available online xxxx

Keywords:
Microgrids
Unit commitment
Economic dispatch
Genetic algorithm
Mixed integer linear programming

ABSTRACT

Energy Management System (EMS) applications of modern power networks like microgrids have to respond to a number of stringent challenges due to current energy revolution. Optimal resource dispatch tasks must be handled with specific regard to the addition of new resource types and the adoption of novel modeling considerations. In addition, due to the comprehensive changes concerning the multi cell grid structure, new policies should be fulfilled via microgrids' EMS. At the same time achieving a variety of (conflicting) goals in different microgrids requires a universal and a multi criteria optimization tool. Few of recent works in this area have considered the different perspectives of network operation with high amount of constraints and decision criteria. In this paper two dispatch-optimizers for a centralized EMS (CEMS) as a universal tool are introduced. An improved real-coded genetic algorithm and an enhanced mixed integer linear programming (MILP) based method have been developed to schedule the unit commitment and economic dispatch of microgrid units. In the proposed methods, network restrictions like voltages and equipment loadings and unit constraints have been considered. The adopted genetic algorithm features a highly flexible set of sub-functions, intelligent convergence behavior, as well as diversified searching approaches and penalty methods for constraint violations. Moreover, a novel method has been introduced to deal with the limitations of the MILP algorithm for handling the non-linear network topology constraints. A new aging model of a Lithium-Ion battery based on an event-driven aging behavior has been introduced. Ultimately, the developed GA-based and MILP-based optimizers have been applied to a test microgrid model under different operation policies, and the functionality of each method has been evaluated and compared together.

1. Introduction

The current worldwide power system transition towards a smart grid paradigm has invoked a wide variety of attempts to integrate environmentally friendly renewable energy sources (RES), distributed dispatchable generators (DDG), energy storage devices, as well as demand side response (DSR) programs into distribution grids [1]. The huge amount of integrated distributed energy resources (DER) units and changes in energy demand introduce a new energy production-consumption pattern in the traditional structure of the energy systems, which results in miscellaneous operational challenges to guarantee balance, stability, predictability and efficiency in the power networks.

One attractive aggregation approach is the microgrid [2,3], which can be adapted to a wide variety of new power network types and market settings. Aside from its capability of switching

* Corresponding author.
E-mail addresses: mohsen.nemati@siemens.com (M. Nemati), martin.braun@uni-kassel.de (M. Braun), stefan.tenbohlen@ieh.uni-stuttgart.de (S. Tenbohlen).

http://dx.doi.org/10.1016/j.apenergy.2017.07.007
0306-2619/

Nomenclature

Acronyms

ASPM	adoptive SPM
BSS	battery storage system
CEMS	centralized EMS
DDG	distributed dispatchable generator
DER	distributed energy resource
DG	diesel generator
DOD	depth of discharge
DTX	Dynamic-Type crossover
ED	economic dispatch
EMS	Energy Management System
EOL	end of lifetime
FC	fuel cell
GA	genetic algorithm
GHG	greenhouse gas
LL	lifetime loss
MG	microgrid
MILP	mixed integer linear programming
MOP	microgrid operation policies
MT	micro gas turbine
OPF	optimal power flow
PR	P-Redispatching
PV	photovoltaic generator
RCGA	real coded GA
RES	renewable energy source
RESC	RES curtailment
SBX	Simulated Binary Crossover
SN	stress-number
SOC	state of charge
SPM	Semi-Probabilistic Mutation
TPX	two point crossover
UC	unit commitment
URC	unit recommitment
VSO	voltage set point optimization
WT	wind turbine

Symbols

P_{FC}	electrical power of FC
v_{ci}, v_{co}	cut-in and cut-out wind velocity
v_r	rated wind speeds
α_k	externality costs of emission type k
β_{ik}	emission factor of generating unit i
K_{Ag}	SOC aging factor for each partial cycle
N_{Pos}	maximum number of possible cycles
W	weighting of different violation types
Vio	amount of violation
T_{amb}	ambient temperature
P_{STC}	module maximum power
E_M	incident irradiance of the modules
E_{STC}	irradiance under standard test conditions
T_M	temperature of the module
ε_{PV}	module-dependent proportionality constant
P_r	turbine rated power

Variables

C_{BSS}	battery aging cost
P_{PV}	output power of PV plant
$P(v)$	power output of wind turbine
$CF_{DG}(P_{DG})$	operation fuel cost of diesel generator
P_{DG}	output active power of diesel generator
$CF_{FC}(P_{FC})$	fuel cost for a fuel cell
$CM_{DG}(P_{DDG})$	maintenance cost
$SUC(DDG)$	startup costs
$SDC(DDG)$	shutdown costs
CEM_{DDG}	cost of the environmental externalities
$C_{Ev}(t)$	cost of event

between grid-tied and islanded operation modes to enhance supply reliability, it also serves as a promising solution for coordinating stakeholder interests and improving network performance [4] such as congestion relief, voltage control, and loss reduction.

Aside from embedded component-level controls for facilitating island transition and stability maintenance, a large proportion of microgrid-specific functionalities should be realized by an onsite Energy Management System (EMS) [5], which not only serves as an economic optimizer but also monitors and adjusts power flows in the local network [6]. In comparison with their transmission level counterparts, microgrid EMS applications with economic optimization targets are generally faced with more stringent network and emission constraints [2,7]. In addition, such optimal resource dispatch tasks in microgrids—namely the unit commitment (UC) and economic dispatch (ED) problem—must also be handled with specific regard to the addition of new resource types (i.e. storage devices [8] and controllable loads [5] etc.) and the adoption of novel modeling considerations. In last years, many works have introduced interesting and practical concepts for intelligent dispatching of integrated DER in the microgrids. Xiaolong et al. introduce in [9] a building based virtual energy storage system model by utilizing the heat storage capability of the building, which is considered in a dynamic economic dispatch model of the microgrid. Boroojeni et al. present in [10] an oblivious routing economic dispatch algorithm for smart power networks, which focuses on the economic dispatch while managing congestion and mitigating power losses.

Due to different multi-facet complexity of the microgrid UC & ED problem, a large number of algorithms have been proposed in recent years to address this new field of interest. Almost all standard solution techniques for the classical UC problem have been further developed and partially adapted to the microgrid application settings, which include Lagrangian relaxation [11], mixed integer linear programming, and meta-heuristic methods such as particle swarm optimization [12] and genetic algorithm. Amini et al. investigate in [6] two decomposition methods namely Lagrangian Relaxation and Augmented Lagrangian Relaxation which are used to solve security constrained economic dispatch. Jingrui et al. present in [13] an optimal day-ahead scheduling model for a microgrid based on a hybrid harmony search algorithm. One of the promising novelties in the mentioned paper is the consideration of the power flow constraints in the optimization process. Luhao et al. propose in [14] an integrated scheduling approach based on robust multi-objective optimization, in order to minimize operation costs and emissions under the worst-case realization of uncertainties.

The GA based optimization methods have many advantages in comparison to other methods. They are commonly applied to solve different combinatorial optimization problems, which usually contain a high number of potential solutions that makes the application of enumeration techniques (e.g. dynamic programming lagrangian relaxation) problematical. Another promising advantage of the GAs is their flexibility and general applicability. The solution region may include continuous or disjoint areas feasible

Please cite this article in press as: Nemati M et al. Optimization of unit commitment and economic dispatch in microgrids based on genetic algorithm and mixed integer linear programming. Appl Energy (2017), http://dx.doi.org/10.1016/j.apenergy.2017.07.007

or infeasible parts. Furthermore, non-linearity of the problem in objective functions or constraints can be handled in the GAs [15]. An important feature of the GAs is their ability of self-optimization and self-healing. In the optimization process, the optimizer settings are autonomously and continuously adapted and the searching zone and focus are adjusted dependent on different defined quality factors.

Mariani et al. investigate in [8] an off-line scheduler for the day-ahead aims at minimizing the cost with regards to the daily energy rates and considering the forecasts for both consumption and production. The optimizer is based on a trust-region method or on a niching genetic algorithm. In [5] a multi-objective genetic algorithm is used to solve a multi-objective model to optimize the time allocation of domestic loads within a planning period of 36 h in a smart grid context. Bei et al. propose in [16] a combined sizing and energy management methodology. The sizing problem is solved using a genetic algorithm. The EMS is formulated as a UC problem and is solved with MILP method.

Due to the high efficiency and modeling flexibility in MILP method as well as the availability of the promising commercial solvers, MILP is used to solve the UC and ED problem in many recent works. Parisio et al. [17] have introduced an optimizer for the EMS based on the MILP, which considers UC, ED of the system. Olivares et al. [18] use MILP to develop a CEMS for an isolated microgrid based on rolling horizon optimization. Wu et al. [19] have developed a high accuracy process based on MILP to optimize a microgrid including diesel generator (DG), fuel cell (FC), microturbine (MT), and battery storage system (BSS) units.

Although many efforts have been made for developing optimization algorithms to manage microgrid operation, few of them [6,10,16] have considered different perspectives of network operation in the same optimization or have provided enough flexibility to work with different networks with a high amount of constraints, decision criteria and objectives. The previous works have improvement potentials and at least one of the following weaknesses and problems:

- Low level of flexibility of the optimizer in order to be utilized for different policies and strategies, and for different kind of microgrids (No universal tools).
- Lack of accuracy in the optimization process (e.g. locking in local optimum).
- Simplification of microgrid component models such as BSS aging model.
- Simplification of non-linear problems for example for combined active and reactive power optimization in distribution grids, or fully neglecting network constraints.
- Absence of enough results validations for optimization methods from different optimization categories used for different case studies.

The general idea behind this present work is to narrow the gaps in the last works with a comprehensive consideration of missing mentioned points, vital constraints and decisive multi-objectives of future microgrids' EMS. The main contributions of this paper include the followings:

1. The developed optimal scheduling is aimed firstly at minimizing the total operation cost comprising day-ahead market transactions, fuel costs, maintenance costs, network losses, and Aging costs, while in the same time trying to minimize GHG emissions of the microgrid.
2. The introduced EMS is also focused on reducing the microgrid's dependency on the main grid and the electricity market, enhancing voltage and power flow quality of the grid, and maximizing the utilization of the renewable energy inside the considered region.
3. A new aging model of the Lithium-Ion battery based on an event-driven aging behavior has been developed and implemented in the investigated EMS. This model considers the impacts of partial cycles and SOC-rate on the BSS life time.
4. Both optimizers are able to consider simultaneously different - sometimes conflicting - objectives and constraints under various microgrid operation modes and policies.
5. This paper introduces a novel method to deal with the limitations of the MILP algorithm for handling network topology constraints. This is achieved by combining the MILP solver with a developed network calculation program.
6. The second optimizer is based on an enhanced real-coded (non-binary) genetic algorithm, which simultaneously solves UC and ED optimization problems. The main novelty of this method lies in incorporating the network constraints impacts in the GA optimization mechanism. In addition, a number of flexible and case-specific sub-operators have been integrated to guarantee a fast convergence and a sufficient diversity of the interim solutions.
7. A comprehensive analysis of different microgrid operation policies based on the quasi-realistic case studies is done. Furthermore, an extensive comparison between MILP and GA results is performed, which shows accuracy, flexibility, and speed of each method. This evaluation focuses on cost-benefit analysis of different microgrid operation policies such as connected and islanded operations, cost-optimized, emission-optimized, and combined modes.

The rest of the paper is organized as follows. Section 2 introduces the technical and economical models of different utilized DER and operational policies in microgrids. In Section 3, the GA-based optimization method is described and different flexible sub-modules and techniques are introduced. MILP-based optimization process and structure of sub-optimizers are explained in Section 4. Section 5 provides results of different case studies and evaluates the functionality of GA and MILP optimizers. Finally, some conclusions are given in Section 6.

Fig. 1.1 illustrates an overview of the developed and discussed parts in this paper.

2. Models and operational policies

The focus of this paper lies on the development and integration of CEMS. The upcoming Section 2.1 deals with the technical, economical and environmental models of the modeled equipments.

2.1. Component models and assumptions in EMS

One important issue, which has a significant effect on decisions in an EMS, is the input-output characteristic of the generators. The technical models are formulated as power input-outputs equations $P_{DER}^{(x)}$ and the economical models are defined as power-cost equations $CF_{DER}(P_{DER})$ as well as maintenance, start-up and shut-down costs. The environmental models are shown as power-externalities' costs $CEM_{DER}(P_{DER})$. For the PV generators, and wind turbines no economical and environmental issues have been taken into account; and their operations are assumed to be free of charge and pollution.

2.1.1. Photovoltaic generator model

Active power output of a PV generator, which depends on the power density of solar irradiation and ambient temperature at PV plant [20], can be calculated as following:

Please cite this article in press as: Nemati M et al. Optimization of unit commitment and economic dispatch in microgrids based on genetic algorithm and mixed integer linear programming. Appl Energy (2017), http://dx.doi.org/10.1016/j.apenergy.2017.07.007

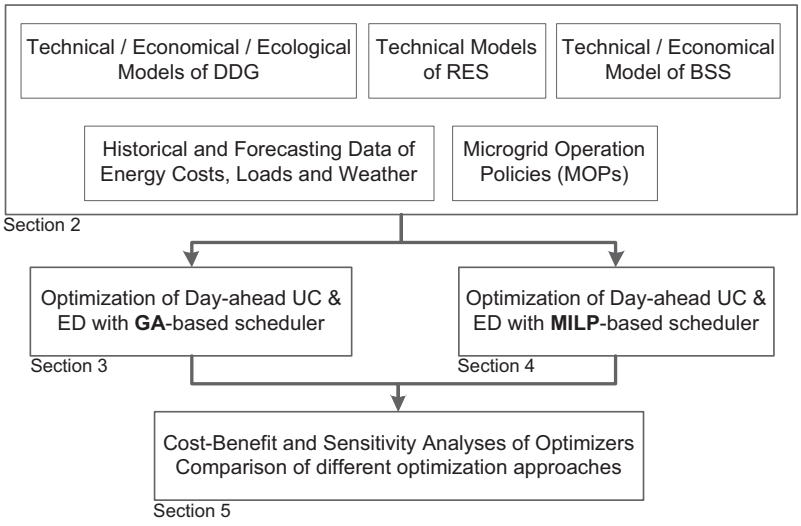

Fig. 1.1. Overview of developed parts and process of the paper.

$$P_{PV}(E_M) = P_{STC} \cdot \frac{n \cdot E_M}{E_{STC}}[1 + k \cdot (T_M - T_{STC})] \tag{2.1}$$

where P_{PV} is the output power of PV plant, P_{STC} is the module maximum power under standard test conditions, n is the number of modules in the plant, E_M is the incident irradiance on the modules, E_{STC} is the irradiance under standard test conditions (1000 W/m^2), k is the temperature coefficient of the power [%/°C], T_M is the temperature of the module [°C] and T_{STC} is the reference temperature [°C]. The factor k is derived from the data sheet of the PV module. The temperature of the module T_M can be approximated depending on T_{amb} and E_{STC} as follows:

$$T_M = T_{amb} + \varepsilon_{PV} \cdot \frac{E_M}{E_{STC}} \tag{2.2}$$

where T_{amb} is the ambient temperature [°C] and ε_{PV} is a module-dependent proportionality constant. Typical values for ε_{PV} and further information about the PV model are given in [21].

2.1.2. Characteristic of the wind turbine model

The power output of a wind turbine depends on aerodynamic characteristic of the turbine and the wind speed v [m/s] at the hub height. Power output of wind turbine is calculated as follows:

$$P(v) = \begin{cases} 0 & for\ v < v_{ci} \\ P_r \cdot \frac{v^3 - v_{ci}^3}{v_r^3 - v_{ci}^3} & for\ v_{ci} < v < v_r \\ P_r & for\ v_r < v < v_{co} \\ 0 & for\ v > v_{co} \end{cases} \tag{2.3}$$

where P_r represents turbine rated power [kW], v_{ci} and v_{co} are the cut-in and cut-out wind velocity, respectively, v and v_r are the actual and rated wind speeds, respectively [22,23].

2.1.3. Diesel generator model

The fuel consumption cost of a DG can be expressed mainly as a quadratic polynomial [24]. The fuel cost of a diesel generator CF_{DG} [€/h] is therefore achieved by multiplying the diesel cost c_{Diesel} by the quadratic function:

$$CF_{DG}(P_{DG}) = c_{Diesel} \cdot (aP_{DG}^2 + bP_{DG} + c) \tag{2.4}$$

where P_{DG} [kW] is the output active power of the diesel generator. The diesel generator cost function parameters, a [l/(kW^2 h)], b [l/(kW h)] and c [l/h], can be obtained from the input/output measurement data taken during "heat run" tests, when the DG is operated with different output-power between its minimum and maximum operation range [25,26]. This data is usually available in the manufacturer's data sheet in form of fuel consumption for 25%, 50%, 75% and full loads.

2.1.4. Fuel cell model

Different technologies of FC operate at maximum. electrical efficiencies from 40% to 60%. According to the studies in [27,28], the maximum efficiency of fuel cells (e.g. Protone Exchange Membrane (PEM-FC)) can be achieved around 10–40% of its full load. The fuel cost $CF_{FC}(P_{FC})$ [€/h] for a fuel cell is calculated as follows:

$$CF_{FC}(P_{FC}) = c_{Gas} \cdot \frac{P_{FC}}{\eta_{FC}} \tag{2.5}$$

where c_{Gas} is the natural gas price, P_{FC} is the net electrical power produced at PCC of FC [kW] and η_{FC} is the FC total efficiency [29].

Substituting the FC efficiency curve, given in the data sheet of the FC, into the Eq. (2.6) results in a quadratic cost function similar to that of DG but with different quadratic parameters:

$$CF_{FC}(P_{FC}) = c_{Gas} \cdot (aP_{FC}^2 + bP_{FC} + c) \tag{2.6}$$

where, a [l/(kW^2 h)], b [l/(kW h)] and c [l/h], are the quadratic function parameters.

2.1.5. Micro gas turbine model

Micro turbine (MT) model is similar to DG and FC models. However, the operation cost function parameters and the curves are adopted in order to model the efficiency and performance of a MT unit [30,31]. Usually, the maximum accessible efficiency of a MT is limited up to 32%. Table 2.1 gives the Parameters of the quadratic operation cost functions of the modeled DDG in this paper and Fig. 2.1 shows the operation cost curves of the units. The natural gas price is assumed equals to 0.09 €/kW h, and the diesel cost is defined equals to1.2 €/l in this paper.

2.1.6. Other operation costs of the DDG

In addition to fuel consumption costs, the DDG cause extra costs like maintenance costs, start-up and shut-down costs, and emission costs. The following defined equations are applicable for each kind of DDG (DG, FC, MT) in this paper, therefore is explained only once here.

Please cite this article in press as: Nemati M et al. Optimization of unit commitment and economic dispatch in microgrids based on genetic algorithm and mixed integer linear programming. Appl Energy (2017), http://dx.doi.org/10.1016/j.apenergy.2017.07.007

Table 2.1
Parameters of the quadratic operation cost functions of the modeled DDG.

Unit	P_{rated} [kW]	a [ml/(kW^2 h)]	b [l/(kW h)]	c [l/h]
DG1 "C55"	40	2	0.194	1.85
DG2 "C90"	70	1.115	0.2232	1.75
FC	50	9.864	2.061	1.152
MT1 "C90"	200	1.924	2.232	82.33
MT2 "C65"	65	–	2.965	32.2

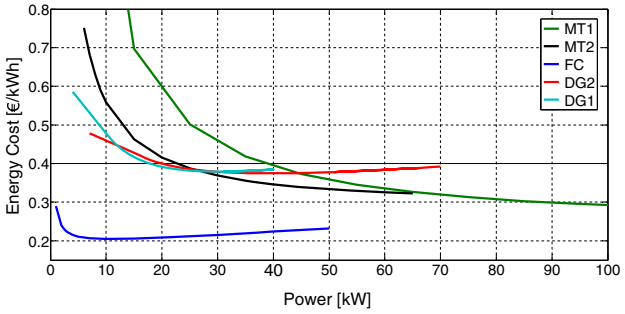

Fig. 2.1. Quadratic operation cost curves of the DDGs.

Maintenance cost: The maintenance cost is usually related directly to the power output. It is assumed to have a proportional relationship with the produced power [P_{DDG}]:

$$CM_{DDG}(P_{DDG}) = c_{DDGMaint} \cdot P_{DDG} \tag{2.7}$$

where the proportionally constant ($c_{DDGMaint}$) for each distributed generator is different. The cost of FC maintaining is assumed to be in the range of 0.004–0.01 €/kW h. The maintenance cost estimation of microturbine units is assumed to be ranging from 0.004 up to 0.015 €/kW h. The maintenance costs of diesel generators vary also in the range of 0.004–0.02 €/kW h [32,33].

Startup and shutdown costs: Using the following simplified equation, the constant SUC and SDC can be defined for the small-scaled DDG:

$$SUC(DDG) = k_{su} \cdot t_{su} \cdot c_{fuel} \cdot \frac{P_{min}}{\eta_{DDG,min}}$$
$$SDC(DDG) = 0.5 \cdot SUC(DDG) \tag{2.8}$$

where $SUC(DDG)$ and $SDC(DDG)$ are the startup and shutdown costs of the DDG [€], k_{su} is the startup consumption factor, t_{su} is startup duration, c_{fuel} is the cost of fuel (diesel or gas) [€], P_{min} is the minimal power output of the unit [kW], and $\eta_{DDG,min}$ is the efficiency of unit by minimum power.

Emission costs: The cost of the environmental externalities (CO_2, SO_2, NO_x) is assumed to be as a linear function of output power (Eq. (2.9)):

$$CEM_{DDG} = \sum_{k=1}^{Nem}\sum_{i=1}^{Ngen} \alpha_k \cdot \beta_{ik} \cdot P_i(t) \tag{2.9}$$

where *Nem* is the number of emission types, α_k is externality costs of emission type k [€/kg], *Ngen* is the number of DDG, β_{ik} is the emission factor of generating unit i and the emission type k [kg/kW h], $P_i(t)$ is the power output from generator i [kW]. Externality costs of main grid generation, FC, MT, and DG units stated in [30,33,34] have been summarized in Table 2.2.

2.1.7. Energy storage system

The Lithium-Ion battery storage system (BSS) has been modeled as the required storage unit for the purposes of economic load shifting, more reliable islanding, peak power shedding and reactive power control. This new model (in microgrid UC/ED field) includes some physical and security limits, dispatching assumptions and policies, operation losses, and aging model parameters (also see [35,36]).

The maximum charge and discharge power of BSS must be limited in the range of loading capacity of the inverter. Furthermore, battery state of charge should be limited between SOC_{Min} and SOC_{Max}, which are fixed as 10% and 90% of the total BSS capacity (Ah capacity).

It is also assumed that the initial SOC of the BSS at the beginning of the dispatching horizon SOC_{Start} is the minimum value (i.e. SOC_{min}), since it results in the best BSS dispatching performance and minimum total operation costs. Moreover, in order to prepare the battery SOC for the next optimization horizon (e.g. next day) and to generalize the optimal dispatching of the system, the final SOC value SOC_{End} should be equal to the starting SOC value SOC_{Start}.

In many works related to the UC and ED of the power systems (e.g. microgrids), the aging of BSS have been neglected or strongly simplified [25,37]. In this work, a new BSS model is integrated into the dispatching model library, which considers aging behavior of the lithium-Ion battery more accurately. The cycle life aging of a battery depends on temperature, depth of discharge (DOD), the number of cycles, and the charging/discharging currents [35].

In the developed BSS model, the following issues are considered:

- The full and partial cycles (events) are counted and weighted to determine the lifetime loss of the battery considering a predefined stress-number (SN) curve. This SN-curve (or Woehler curve [38]), which is given by some manufacturers in the data sheet, shows the possible number of (partial) cycles of a BSS as a function of DOD until the end of lifetime (EOL) (e.g. 80% state of health).
- Two types of partial cycles, namely micro-cycles and macro-cycles can be taken into account.
- A micro-cycle is started and terminated by local minimum or maximum SOC values during a charging or discharging process.
- A macro-cycle is considered here as a combination of some micro-cycles (at least three) and represents the process between the global extremes of the SOC trend curve.

For each partial (micro/macro) cycle, the number of expected cycles in BSS life time and consequently lifetime loss (LL) is calculated (Eq. (2.10)) using the following Woehler curve [36,39], illustrated in Fig. 2.2. The blue[1] curve shows the number of expected cycles (N_{POS}) in battery life time depending on DOD and the red curve shows equivalent full cycles in BSS operation.

If $N_{Evk,max}$ is the maximum number of events (micro- and macro-cycles) k that can happen during the lifetime of a BSS until EOL (assuming that only events of type k occur) and N_{Evk} is the number of events k, that have occurred during the operation period, then the loss of lifetime associated with event k is:

$$LL_k = \frac{N_{Evk}}{N_{Evk,max}} \qquad LL = \sum_k LL_k \tag{2.10}$$

The EOL is reached when LL is equal to 1. Also the cost of events can be calculated as follows:

$$C_{Ev}(t) = 0.5 \cdot LL(t) \cdot Cap_{BSS} \cdot C_{inv} \tag{2.11}$$

where Cap_{BSS} represents the capacity of BSS [kW h], C_{inv} is the investment cost for battery bank.

[1] For interpretation of color in Figs. 2.2, 5.3 and 5.12, the reader is referred to the web version of this article.

Please cite this article in press as: Nemati M et al. Optimization of unit commitment and economic dispatch in microgrids based on genetic algorithm and mixed integer linear programming. Appl Energy (2017), http://dx.doi.org/10.1016/j.apenergy.2017.07.007

Table 2.2
Parameters of the externality costs and the emission factors of the main grid generation, FC, MT and DG units.

Emission Type	External Costs [€/kg]	DG [kg/MW h]	FC [kg/MW h]	MT [kg/MW h]	Main Grid [kg/MW h]
CO_2	0.0275	0.6495	0.4889	0.7239	0.8891
SO_2	1.9475	0.2059	0.0027	0.0036	1.8016
NO_x	8.2625	9.8883	0.0136	0.1995	1.6021

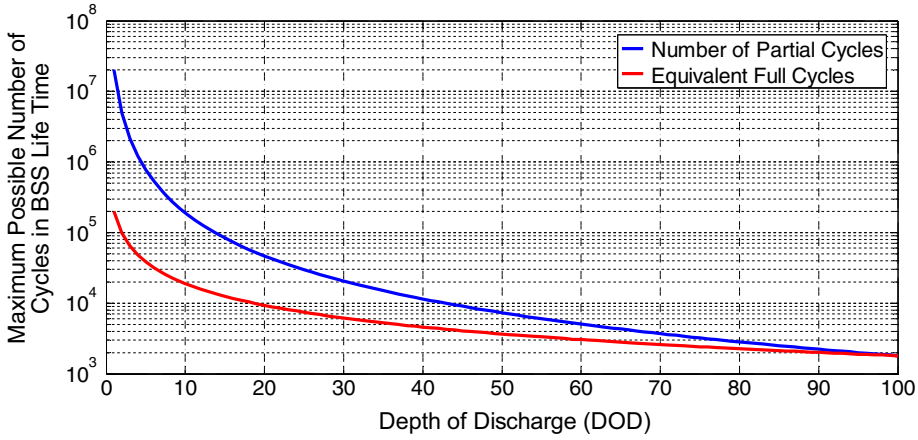

Fig. 2.2. Stress number (SN) curve of a lithium-Ion battery – Maximum possible number of cycles in BSS life time dependent of the DOD [36,39].

Moreover, the SOC of the battery also has a major influence on the aging process. Gerschler has proved in [35], that the lifetime loss of an event (micro/macro cycle) rises non-linearly with an increasing SOC because higher SOC causes more interior stress in the battery cells. Fig. 2.3, which is calculated and adopted curve from [35], illustrates the SOC aging factor curve (K_{Ag}) for a Lithium-Ion battery.

With considering both of SN-curve and SOC aging factor curve, the battery aging cost in total observation time can be calculated as (2.12):

$$C_{BSS} = 0.5 \cdot Cap_{BSS} \cdot C_{Inv} \cdot \sum_{i=1}^{N} \frac{K_{Ag,i}(SOC)}{N_{Pos,i}(DOD)} \tag{2.12}$$

where C_{BSS} is the battery aging cost, N is the number of considered micro- and macro-cycles (events) in battery operation period, K_{Ag} is SOC aging factor for each partial cycle dependent on average SOC of each event, and N_{Pos} is maximum number of possible cycles in BSS life time.

Related to the BSS aging costs in microgrid dispatching, different settings for level of aging cost consideration will be used. Level 1 means consideration of operation costs of microgrid without regarding any aging cost. Level 2 refers to the cost of micro-cycles added to costs of the level 1. Aging level 3 means that the cost of macro-cycles are added to the costs of the level 2, and finally level 4 means that all operation costs and aging factors and costs (inclusive SOC-factor) will be considered in BSS aging model.

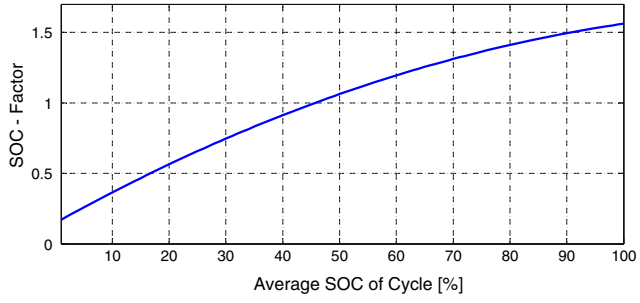

Fig. 2.3. SOC Aging Factor for a lithium-ion battery, considered in lifetime loss of events.

2.2. Microgrid operation policies

Five main operation policies (MOPs) are defined and subsequently considered in the optimization process (see Fig. 2.4) [40,41].

Cost-effective operation (MOP 1): The objective function is the minimization of the operation and the aging costs of the microgrid components. Due to the main focus on the optimization of MG costs, power flow quality (voltages improvement and congestion management) and emission reduction will be neglected here.

$$\text{Min}\left\{C_{MOP1} = \sum_{t=1}^{n}\sum_{i=1}^{Ngen}[CF_{DDG,i,t} + CM_{DDG,i,t} + SUC_{DDG,i,t} + SDC_{DDG,i,t}] + C_{BSS,t} + C_{Ex,t}\right\} \tag{2.13}$$

where C_{MOP1} is the total MG cost for n hours under MOP1, $Ngen$ is the number of DDG, $CF_{DDG,i,t}$ is DDG fuel consumption costs, $CM_{DG,i,t}$ is DDG maintenance costs, $SUC_{DG,i,t}$ and $SDC_{DG,i,t}$ are startup and shutdown costs, $C_{BSS,t}$ is total battery aging costs (including micro/macro cycles and SOC-factor), and $C_{Ex,t}$ is costs/revenues of purchasing/selling energy.

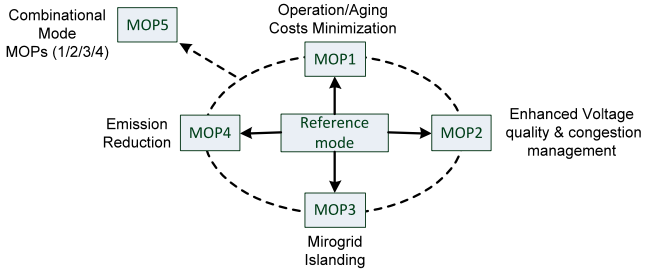

Fig. 2.4. Overview of the defined microgrid operation policies.

Please cite this article in press as: Nemati M et al. Optimization of unit commitment and economic dispatch in microgrids based on genetic algorithm and mixed integer linear programming. Appl Energy (2017), http://dx.doi.org/10.1016/j.apenergy.2017.07.007

Grid supporting mode (MOP 2): In grid-supporting operation, the optimizer conducts many load flow calculations in order to find the possible optimal power flow (OPF) in the MG. Because of higher power quality expectations or critical situation of the microgrid or main grid, controllable units should participate actively in different ancillary services like minimization of grid losses, enhancement of voltage quality (maintaining voltage limits), and elimination of system congestion either inside microgrid or at connection points with external grids. DDG aging constraints (ramp rates and minimum Up/Down times) will be neglected and battery costs $C_{BSS,t}$ will be diminished to level 1.

Maximum islanding degree (MOP 3): In this case, either there is no physical connection (e.g. opened connection switch) with macro-grid, or no power will be exchanged, or only a fixed and predefined power profile may be considered as exchange power. Formulation of the objective function is again similar to MOP1 objective function, but only the term $C_{Ex,t}$ is fixed (0 or fixed). The aging costs (DDG and BSS) will be neglected (like MOP2), and power flow quality issues will be ignored (similar to MOP1) because there is no focus on the aging cost minimization.

Eco-friendly operation (MOP 4): In this mode, the objective function can be formulated as the minimization of the pollutant treatment costs as follows:

$$\mathrm{Min}\left\{C_{MOP4} = CEM_{system} = \sum_{k=1}^{Nem}\alpha_k \cdot \left(\beta_{Grid,k}\cdot P_{Grid}(t) + \sum_{i=1}^{Ngen}\beta_{ik}\cdot P_i(t)\right)\right\} \tag{2.14}$$

where CEM_{system} is the total emission costs of the system (MG and main grid), *Nem* is the number of emission types, α_k is externality costs of emission type k [€/kg], $\beta_{Grid,k}$ is the emission factor of main grid [kg/kW h], P_{Grid} is the injected power from main grid [kW], *Ngen* is the number of DDG, β_{ik} is the emission factor of the generating unit i and the emission type k [kg/kW h].

Multifunctional policy (MOP 5): In multi-objective concept, the operation strategies of the previous four MOPs will be combined in order to partly satisfy different stakeholders and to achieve a moderate operation. Top priority is given to reliability, supporting the grid and unit constraints, i.e. power balance (islanded mode), avoiding voltage violations and congestions and all the limitations of the DDG/BSS.

$$\mathrm{Min}\{C_{MOP5} = \kappa \cdot R_{sum/MOP1}\cdot C_{MOP1} + \gamma \cdot R_{sum/MOP4}\cdot C_{MOP4}\}$$

$$\kappa + \gamma = 1 \quad \kappa,\gamma \in [01]$$

$$R_{sum/MOP1} = \frac{CF_{DDG,i,t} + C_{Ex,t} + CEM_{system}}{CF_{DG,i,t} + C_{Ex,t}} \tag{2.15}$$

$$R_{sum/MOP4} = \frac{CF_{DDG,i,t} + C_{Ex,t} + CEM_{system}}{CEM_{system}}$$

where C_{MOP5} is the combined operation, aging and emission costs, κ and γ are weighting factors for C_{MOP1} and C_{MOP4} combination. $R_{sum/MOP1}$ and $R_{sum/MOP4}$ $\mathrm{Ratio}_{\mathrm{CostDiversity}}$ are constant parameters, which are calculated in rated power of all generators and applied to level the operation and emission costs. CF_{DDGs} is sum of the DDG operational cost, C_{Ex} is the sum of cost of the imported energy from main grid, and CEM_{system} is the sum of system emission costs.

Reference mode (REF): In this mode, some DDG constraints related to aging (ramp rates and min. Up/Down times) will be neglected and considered battery costs $C_{BSS,t}$ will be diminished to level 1 (without aging costs). In addition, no voltage and loading constraints are considered in this mode. Also microgrid operates in a normal connected mode. The objective function is only the minimization of operation costs of the microgrid components. The formulation of the objective function remains the same as the MOP1 objective function without including any aging costs.

3. Optimization of the microgrids' UC and ED with genetic algorithm

3.1. Genetic algorithm process for UC & ED

In this work a real coded GA (RCGA) is developed and modified for optimization of the UC and ED of the microgrid units (see also author's publications [42–44]). In this way, the structure of a GA (genes, chromosomes, generation's process, evaluations, etc.) is adjusted to this problem. Each gene contains the information about status of a unit and the value of its active and reactive powers for a certain time step, while each chromosome includes the active and reactive power of a unit for the whole optimization horizon. Furthermore, each individual representing the characteristics of its chromosomes contains the information about all units in the microgrid in the entire optimization horizon. Fig. 3.1 shows an overview of the GA optimization process in this work. The optimization process consists of three major sections:

1. *Input data and initial preparations:* Firstly, the inputs are prepared and imported containing the settings and parameterizations of the algorithm, component models information and the microgrid's fixed inputs like load curves, etc. These data are processed and encoded in the RCGA language. Then, the first population is created and first power flow calculation based on first population is executed.
2. *Population reproduction:* The populations are reproduced (genotype-part). The first generation is initialized based on an adopted priority list method. Through ranking and selection of some individuals from the last population and the recombination and the mutation of these candidates, the populations of the next generations are produced.
3. *Population evaluation:* Afterwards, the individuals are transformed to real-world values (decoded to kW and kvar), simulated (with one power flow calculation per each individual) and evaluated (phenotype-part) during assigning the values of objective function, and fitness function. Best solutions are sent further to stop-criterion in order to build the next generation components or stop the algorithm.

In the coming sections, a closer look will be taken at the functionality of each of the above-mentioned steps and the subfunctions of the algorithm.

3.2. First population initialization based on priority list method

In this new initialization method, the population is not generated fully random; on the contrary, the population is adjusted to the UC/ED problem without (too much) limiting the search space. The aim of this method is assigning a reasonable probability to each DDG to be online in a time step and a time span based on priority list method [45]. The major challenge is due to considering minimum on- and off- time of the DDG. With random initialization of GA too many constraint-violations may occurr, which cannot be solved until the last generations in GA process.

First of all, the microgrid units are listed in relation to their energy costs and rated powers. For calculation of the utilization (ON status) probability of the units, three possible criteria can be taken into consideration. The first criterion is the satisfaction of the microgrid demand. The second one is the export electricity price (cheaper DDG may sell energy to macro-grid) and the last one is the maximum possible exchange power of microgrid. In this

Please cite this article in press as: Nemati M et al. Optimization of unit commitment and economic dispatch in microgrids based on genetic algorithm and mixed integer linear programming. Appl Energy (2017), http://dx.doi.org/10.1016/j.apenergy.2017.07.007

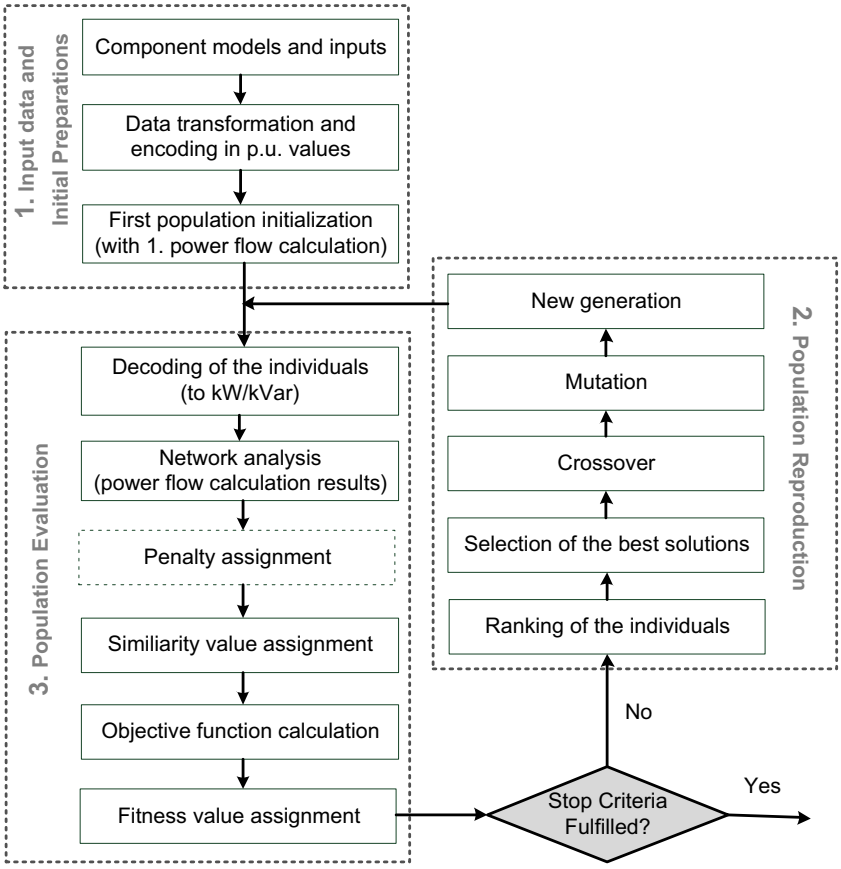

Fig. 3.1. The optimization process of developed genetic algorithm for microgrids' UC & ED.

manner, two groups of DDG can be defined, namely the high priority and the low priority, which get a discrete spectrum of activation probabilities. Because of the minimum up/down-time constraints, not only the probabilities in single time step should be assigned, but also the probabilities for the following time steps should be considered.

For defining the reactive power of the DDG and BSS in the initial population, the reactive power of the loads and the potential voltage violations must be taken into consideration. As a first step, the average power factor of the loads of each time step is calculated and the power factors of units (DER and BSS) are regulated with the increased probabilities to compensate the reactive power demand of the loads. If a voltage violation is probable the reactive power output of the units at the node and neighboring nodes is adjusted.

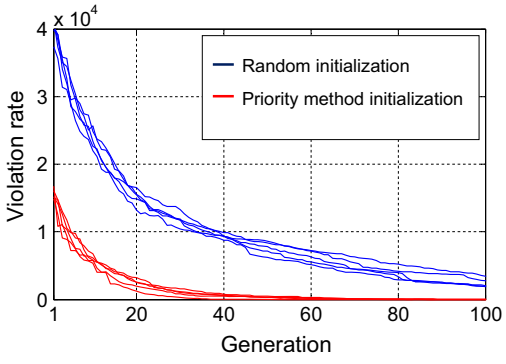

Fig. 3.2. The process of violation rate (penalty) during the first 100 generations for five successful tests for the randomly initialization vs. the priority list initialization.

Fig. 3.2 shows the process of the violation rate (penalty) during the first 100 generations for five successful tests for GA with randomly initialization and with priority list initialization methods. The initial violation rate in randomly initialization is almost three times higher than the other case.

After about 70 generations the violations in priority method converge to zero, but about 20% of violations of random initialization method (all 10 tests) still exist.

3.3. Ranking and selection of the individuals

After evaluating the population of the last generation, a new population should be produced by different GA-operators. First of all, the individuals are sorted according to their fitness values. The selection probability is assigned to the individuals depending on their ranks. Once the individuals were ranked, the appropriate ones will be chosen in a semi-randomly manner. For producing the new offspring, these candidates will either be permeated directly to the next generation with elitism selection or will be used in the next GA-operators via tournament selection. In the context of GA, elitism is referred to finding the best solutions through the population which is able to survive to the next generation. In tournament selection, in each generation k individuals are picked randomly from the population and compared with each other in a *tournament*. The winner of this competition will then enter the mating pool. This process is repeated until the mating pool is complete and ready for GA-operators (crossover and mutation).

Please cite this article in press as: Nemati M et al. Optimization of unit commitment and economic dispatch in microgrids based on genetic algorithm and mixed integer linear programming. Appl Energy (2017), http://dx.doi.org/10.1016/j.apenergy.2017.07.007

3.4. Crossover methods

After completing the mating pool by means of the tournament and elitism selections, the crossover operator starts to recombine the individuals in the pool and generates a new population. The information of an individual is represented by chromosomes consisting of genes. The crossover rate determines which proportion of the parental chromosomes should be recombined.

Simulated Binary Crossover (SBX): In the SBX method [46], values going beyond the space (values) between the parental values are produced. A probability distribution centering the parent solutions is considered and two children solutions are created on this probability distribution. At the beginning of GA-process, parent solutions are expected to be very diverse and the solutions may be very distantly. But in last generations, the search converges towards a solution and parents become similar and children solutions also become more similar to the parent solutions.

In UC/ED problems, SBX defines only the values of the active/reactive powers but not the status of the DDG. The DDG-status (on/off) of the children is determined by the status of the parents, through a binary single or two point crossover (SPX and TPX) [24,26]. If the status of a unit is on, the value of the SBX is used; otherwise the unit stays off.

Dynamic-Type crossover (DTX): While the SPX and TPX crossovers are simple and more reliable and focus on parents' values [24,26], the SBX crossover ensures more diversity and searching ability in GA-process. The feature of SBX has a major effect on the results in the first generations; also the advantages of SPX (or TPX) can be utilized in finishing generations. In DTX, the GA starts with SBX method and after some generations (e.g. 70%) changes to use simple methods, so it can focus on the best individuals at final generations.

3.5. Mutation process

This GA-operator is used to alter the individuals randomly and maintain a genetic diversity through the generations. A user-defined factor determines the probability of mutation occurrence. The setting of the mutation rate is more critical than that of the crossover rate. If it is set too high, the search will turn into a primitive random search, and if it is set too low the diversity of the search will be worsened. In the usual mutation method a portion of the individuals is randomly selected considering mutation rate and are altered in a bounded range (e.g. active power between max./min. constraints). Since the mutations of different genes happen without considering the other genes, it easily leads to a high mismatch in power balance in islanded grid and to minimum up/down time constraints violations. As a consequence of these violations, the GA stays too long in the unfeasible area. Fig. 3.3 shows the violation rate process of five tests in the reference microgrid using random mutation.

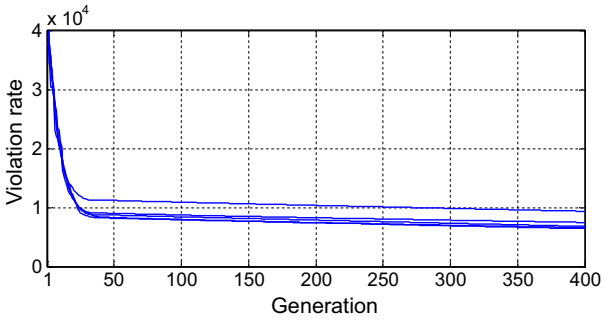

Fig. 3.3. Violation rate (penalties) process in five optimization tests using random mutation.

In this paper, two methods are introduced and tested. The first method introduces a Semi-Probabilistic Mutation (SPM) process adjusted to this problem in MG, and the second method is an adop tive-semi-probabilistic-mutation method based on the first method.

Semi-Probabilistic Mutation Method (SPM): In the procedure of the SPM, through consideration of some critical constraints of microgrids, such as the minimum up/down time of DDG, the power balance, and the voltage violations, the mutation process is (selectively) limited and regulated. This mutation operator contains two modules:

SPM $_{status}$: The initial idea of SPM $_{status}$ has been inspired from [47]. In this generic module, many status-mutation cases, which can lead to minimum up/down time violations, are prevented. Several different mechanisms (rules) are applied for the possible cases, which are dependent on the minimum up/down time constraint value (e.g. 2, 3, 4 h) as well as on the initial state of DDG before the status-mutation process. The developed cases and restrictions in SPM become more essential at the advanced generations, where the false status of mutations can affect the feasibility and convergence of the solutions severely. It is very important to categorize and consider all occurring cases in SPM properly, since an incomprehensive (e.g. with missing occurring cases in UC of DDG) SPM can confine the GA search process unnecessarily and lead to high distance from the global optimum space.

SPM $_{power}$: The SPM $_{status}$ can cause other violations like microgrid power exchange or balance violations and voltage violations. For this reason, another module has been developed, in order to mutate the dispatching of the online DDG and to compensate the active and reactive powers of the mutated units in SPM $_{status}$.

In the first step, considering the mutation rate for dispatching, a portion of individuals is randomly selected to be mutated. In next step, the active power and the reactive power of the online units in selected individuals are mutated as follows.

$$X_{After} = X_{Before} \cdot \left(0.5 + \frac{Gen_{Num}}{Gen_{Max}} \cdot 0.3 + \left(1 - \frac{Gen_{Num}}{Gen_{Max}} \cdot 0.6\right) \cdot rand\right) \tag{3.1}$$

where X_{Before} and X_{After} are the power values before and after the mutation, Gen_{Num} is the current generation number, Gen_{Max} is the maximum number of generations and *rand* is a random number between zero and one. Also, the parameters 0.5, 0.3 and 0.6 are tuned empirically. By this means, each gene (active and reactive power of an online unit in a certain time step) of the selected individuals is mutated between 20% and 50% of its original value considering active and reactive powers capabilities of the unit. The exact mutation value is dependent on the random factor and the number of current generation. That means, the mutation range will be narrowed in last generations, since the convergence should be guaranteed at the final generations.

In the third step, a power compensation process should be conducted for the individuals, which are selected and mutated in SPM_{status}. When a unit becomes online, a random power value is assigned to it firstly. This change in the UC and the power balance in a time step can cause a mismatch of power in the microgrid (especially in islanded mode). Therefore, the generated power of this unit is compensated with a randomly selected online unit. If the power reduction of the selected unit is not sufficient enough to keep the balance between generation and demand, the next online unit is selected randomly and adjusted in order to compensate the remained power unbalance. In the case of UC mutation from online to offline status, a similar process is executed, where the power of other online units are increased to compensate the power deficit.

Please cite this article in press as: Nemati M et al. Optimization of unit commitment and economic dispatch in microgrids based on genetic algorithm and mixed integer linear programming. Appl Energy (2017), http://dx.doi.org/10.1016/j.apenergy.2017.07.007

In the last mechanism, the RES units should be curtailed in case of overvoltages in the microgrid. So that the mutation rate for the units in critical nodes or neighboring nodes is increased. Having performed the necessary corrections of the voltage violations, the RES mutation rate stays high for some generations (e.g. 30 generations), in order to find a technical and economical optimal state. Afterwards, it will be reduced again to reduce the likelihood of the mutation of the good individuals and to keep the best individual (without voltage violation).

Adoptive semi probabilistic mutation (ASPM): In the SPM, the mutation rate (occurrence probability) does not change during the whole optimization time. As another promising approach, the mutation rate can be regulated during generations by using a fuzzy rule mechanism [48]. The mutation probability should be increased when the constraint violations are too high or when the diversity of the population is too low.

3.6. Penalty function

In the concept of penalty assignment method a constrained-optimization problem is transformed into an unconstrained problem by adding a certain value to the objective function based on the constraint violations in a certain individual. The penalty function here contains seven parts:

$$Penalty = [W_P Vio_P + W_Q Vio_Q + W_S Vio_S] + W_{Sw.} Vio_{Sw} + W_R Vio_R + W_V Vio_V + W_I Vio_I \quad (3.2)$$

where W and Vio represent weightings of different violation types (sum of violations in an individual), respectively. P, Q and S are the exchanged active, reactive and apparent powers within the main grid, respectively. Sw is derived from switching and is related to minimum up/down time constraints. R, V and I are ramp rates, voltage and current constraints.

If the penalty weighting factors are set too high and the optimum lies at the boundary of the feasible region, the GA will be pushed deep inside the feasible region very quickly. On the other hand, if the weighting factors are too low, most of the search time will be spent deep in infeasible region because the penalty values are negligible in comparison with value of objective function.

If the number of a certain violation type (e.g. switch) in the fittest individual does not decrease with the progress of the generations, the weighting factor is raised to enforce the reduction of the violations. On the other hand, if it decreases significantly the factor is also reduced to promote the search at the borders to infeasible areas in the search space. Different functions can be implemented to adjust the penalty weighting factors. A continuous adoption function is used to adjust the weighting factors:

$$W_{k+5} = W_k \left(\frac{V_{k+5}}{0.95 \cdot V_k + 0.01} \right) + \frac{0.3 + V_{k+5}}{1 + V_{k+5}} \quad (3.3)$$

where V_k and V_{k+5} are the violations values in generation k and in generation $k+5$, and W_k and W_{k+5} are weighting factors in generation k and generation $k+5$.

3.7. Similarity function

Based on the fitness sharing method, the similarity of an individual to the rest of the population is calculated and, individuals with different UC solutions are favored and supported. In this procedure, an array called *similarity degree* is defined, which counts the number of individuals with the same online DDG in a certain time step. The function computes the similarity degree of each individual by adding all values from this array together, when the individual itself is on. It means that the similarity rate of an individual will be high if its units are active at the time steps in which many other individuals have same online units. The same process is conducted for offline DDG.

3.8. Fitness function assignment

The fitness function that should be minimized in the optimization process, consists of three important mentioned functions, namely objective, penalty and similarity functions. A combination of these functions as fitness function evaluates the quality of solutions (individuals):

$$Fitness = Objective + R_{Ob/Pen} \cdot W_{Pen} \cdot Penalty + R_{Ob/Sim} \cdot W_{Sim} \cdot Similarity \quad (3.4)$$

where W_{Pen} and W_{Sim} are the weighting factors of the penalty and similarity functions. The ratios $R_{Ob/Pen}$ and $R_{Ob/Sim}$ are used to weight the values of these three functions. The objective function is dependent on the selected MOP (see Section 2.2). In each generation, the mean values of these three functions are calculated for the whole population. Afterwards, $R_{Ob/Pen}$ and $R_{Ob/Sim}$ are calculated as follows in order to level the values of the functions:

$$R_{Ob/Pen} = \frac{mean(Objective)}{mean(Penalty)}$$
$$R_{Ob/Sim} = \frac{mean(Objective)}{mean(Similarity)} \quad (3.5)$$

After evaluation of the fitness values, the adjusted stop criteria must be checked. Depending on the analysis type, different stop criteria such as number of generations, maximum optimization time, solution enhancement rate, and unsuccessful tries numbers can be considered.

4. MILP-based optimizer for microgrid EMS

In this paper, an effective method is used to deal with the limitations of the MILP algorithm for handling the topology constraints. This is achieved by the decomposition of the MINLP problem into a MILP-based UC/ED problem and a non-linear network optimization problem. The overall optimization approach is illustrated in Fig. 4.1.

All the inputs, constraints and strategies are formulated firstly as a MILP problem with user-defined algorithm settings and subsequently interfaced to the CPLEX optimizer.

The key to formulate this problem into a MILP form is to linearize the non-linear cost functions in a piecewise manner. Many previous works [17–19] deal with the formulation and simplification of the UC and ED problems to a mixed integer linear programming problem. The initial UC and ED without any network constraints considerations will be performed in this context.

Then the temporary P-set points are imported into power flow calculation (PFC) module using MATPOWER. As an initial result of PFC module output, the calculated network losses will be returned back into the MILP module to initiate a new P-dispatch considering the losses. In the PFC module, the Q-dispatch of the DER units is carried out based on a Q-V droop control considering the power factor limitations. In the default case, all voltage set points of Q-dispatchable generators are adjusted to 1.0. Afterwards, resulting power flow as well as the voltage and loading conditions will be checked. If no violations are detected these P-Q-set points will be accepted as the optimal dispatch results.

If grid voltages in certain nodes deviate from the predefined limits, the voltage set points of the DER with higher Q-injecting-capability will be changed to solve the problem initially with reactive power control (VSO). The DDG voltage set point variation band and the number of DDG can also be predetermined for the Q-optimization

Please cite this article in press as: Nemati M et al. Optimization of unit commitment and economic dispatch in microgrids based on genetic algorithm and mixed integer linear programming. Appl Energy (2017), http://dx.doi.org/10.1016/j.apenergy.2017.07.007

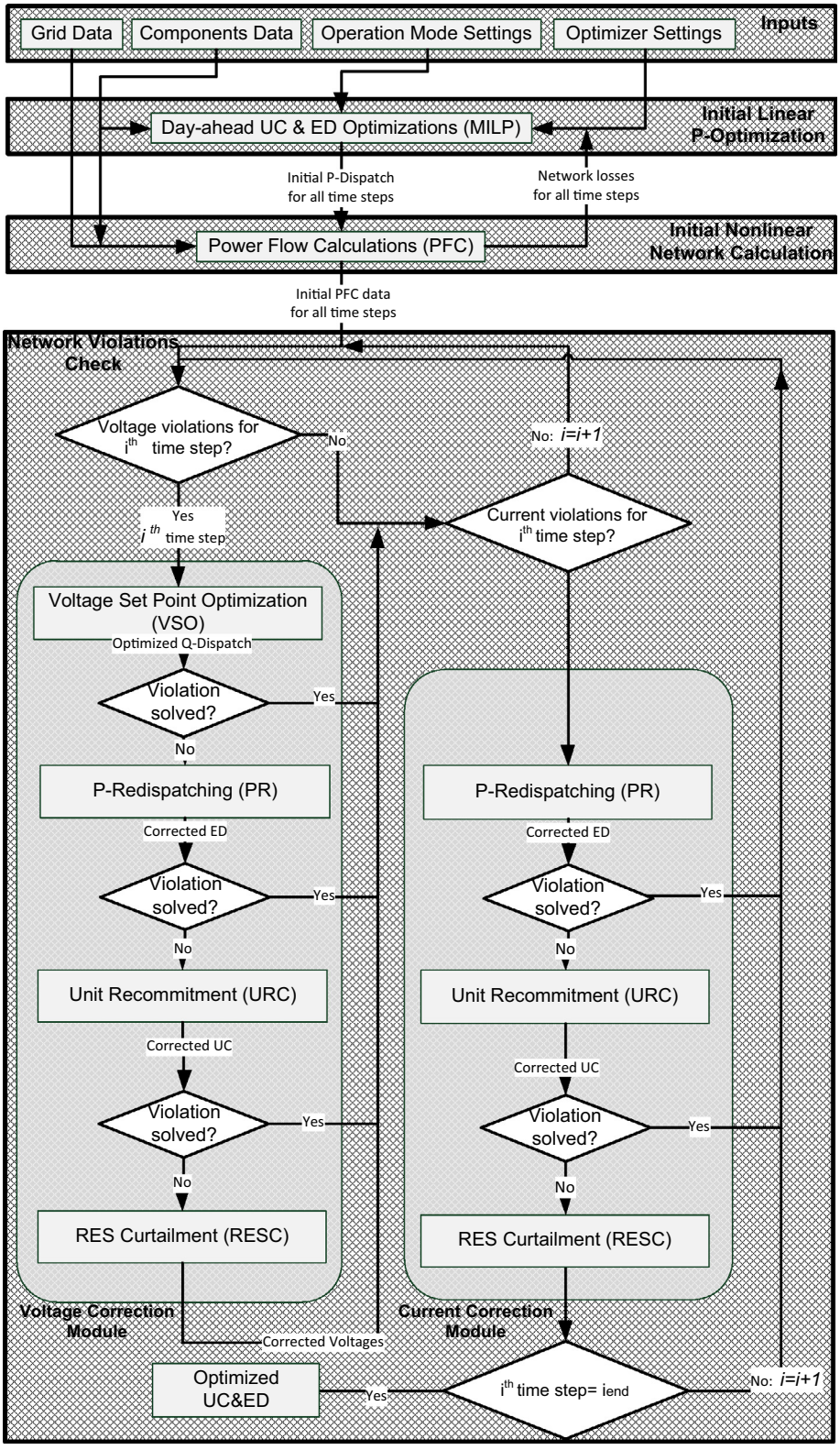

Fig. 4.1. Detailed framework of different optimization modules in MILP-based optimizer.

If the voltage violations in the grid persist despite the VSO adjustment, a P-Redispatching module (PR) will come into effect in order to modify the active power outputs of the DDG units located close to the node with the voltage violation issue. The modified DDG active power outputs will be returned to the MILP module as a fixed and enforced value to be integrated in a new round of UC and ED calculation. This iterative process will be executed up to a point in which either the violation issue is resolved, or the P-limits of DDG are reached.

If the voltage set point variation and the P-Redispatching of already active (ON) DDG are still not sufficient for solving the voltage problem, the unit recommitment module (URC) will be called to switch on a new (offline) generator in the microgrid to meet the network constraints. A set of DDG close to the node with the

Please cite this article in press as: Nemati M et al. Optimization of unit commitment and economic dispatch in microgrids based on genetic algorithm and mixed integer linear programming. Appl Energy (2017), http://dx.doi.org/10.1016/j.apenergy.2017.07.007

minimum voltage value will be consecutively started up and go through the URC process until the problem is solved. Among all of the feasible results, the cheapest solution as the optimal URC decision will be adopted. Apparently, the forced start-up of a new generator in MILP leads to a whole new round of UC, ED and PFC.

If an overvoltage event cannot be resolved via all the pre-mentioned methods, it will eventually be fixed by RES (PV or Wind) curtailment (RESC) implementation for the units located close to the node with the highest voltage.

4.1. Linear optimization core

The mixed integer linear programming problem is formulated in four main parts. On the one hand, the linearized objective function as follows:

$$Maximize\ or\ Minimize(f^T \cdot x) \tag{4.1}$$

where x is the solution vector (e.g. active power of the units) and f^T is the constants to define the MILP objective function. Also three constraint categories for the problem must be formulated:

$$Aeq \cdot x = Beq \qquad lb \leqslant x \leqslant ub \quad A \cdot x \leqslant B \tag{4.2}$$

where Aeq and Beq are the matrixes for formulation of the equality constraints; lb and ub are define the minimum and maximum active powers of the units, respectively; and the matrixes A and B formulate the inequality constraints for the MILP optimizer which are the more important boundaries These are constraints regarding the maximal exchange power with the upstream network, operation constraints like maximum and minimum active powers, maximum ramp up and ramp down rates, minimum up- and down-times and also some constraints for storage devices.

Since the MILP problem formulation only supports linear objective functions, this cost function is piecewise linearized into segments with linear slopes (see Fig. 4.2). The number of segments has a major influence on the optimization time and a minor effect on the accuracy of the calculations in this case. Fig. 4.2 illustrates the trend of calculation time and accuracy for twelve segments in the CPLEX solver. The results of this test case are related to UC and ED of a test microgrid introduced in Section 5.

As can be seen, the computing time stays in a reasonable scale up to seven segments, whereas the optimal cost is not reduced considerably. As a compromise, four segments are used here.

4.2. Initial power flow calculation module (PFC)

Having done the P-optimization by MILP, the P-set points of the units are imported to the PFC module, in order to calculate the voltage, current, optimal Q-Dispatching, and network losses. The PFC module deploys the MATPOWER tool to calculate the power flow based on Newton-Raphson method.

In default mode, the voltage set point is 1.0 p.u., which should be readjusted under critical cases. One of the important aims of the PFC is the network loss calculation. Calculated losses are returned back to MILP where they are regarded as an extra load. Afterwards a new optimal P-Dispatching is conducted. The difference between the P-dispatching in MILP and MATPOWER is only an active power difference at the slack bus.

4.3. Voltage set point optimization (VSO) and Q-redispatching

If any voltage violations occur after the initial PFC, the Q-dispatching should be readjusted to enhance the voltage quality. VSO has been prioritized as the first voltage improvement issue in this optimizer, since the Q-redispatching increases the operational cost less than other options and does not change the optimal P-dispatching significantly. Q-V droops with voltage set points are defined for all types of DER (Fig. 4.3). In order to optimize the Q-dispatch of the DER, the V-Q is shifted up or down in a stepwise manner. In order to redispatch the reactive power of the units, the predefined voltage set points (1.0 pu) must be readjusted. As the first approach, a ranking of the DER according to their Q-potential in a descending order is made. Then, considering a predefined voltage set point band and set point step sizes in inputs, the possible DER voltage set points will be prepared.

For example, a voltage set point band of 0.98 pu to 1.02 pu with a step size of 0.01 pu leads to the possible set point vector of $[0.98, 0.99, 1.00, 1.01, 1.02]$. Now the set points of DER can be varied through defined vector, which lead to different combinations of DER voltage set points. The slope of the units can be set dependent on the voltage set points' space and maximum possible inductive and capacitive powers. For each combination of the set points a

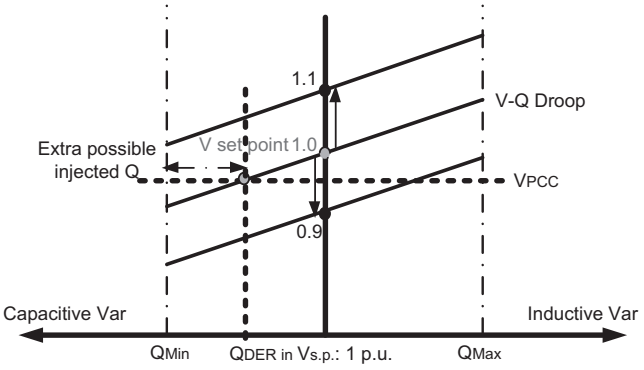

Fig. 4.3. Voltage set point adjustment based on V-Q droop characteristic of DER. The V-Q droop can be shifted up or down to change Q-dispatch of the DER.

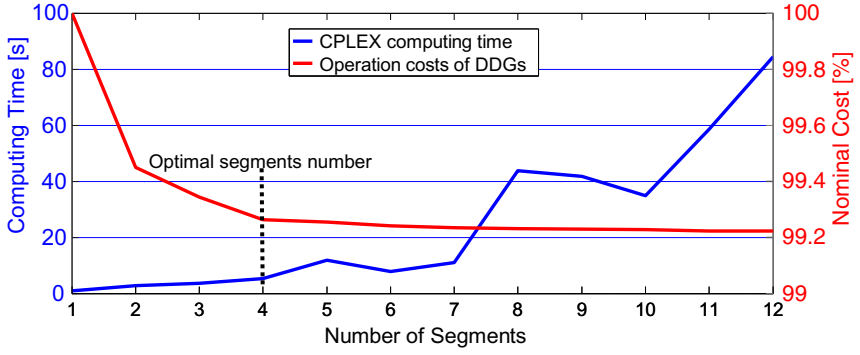

Fig. 4.2. The influence of the linearization's segments number on the computing time and nominal operation costs of a sample microgrid with five DDG.

Please cite this article in press as: Nemati M et al. Optimization of unit commitment and economic dispatch in microgrids based on genetic algorithm and mixed integer linear programming. Appl Energy (2017), http://dx.doi.org/10.1016/j.apenergy.2017.07.007

PFC will be performed. After executing all PFCs, the voltage results are saved in a PFC evaluator unit, where the best set point combination with minimal voltage deviation will be selected.

4.4. P-Redispatching module (PR)

The PR manipulates the P-dispatching of the certain DDG optimized by the MILP, which can be effective for the voltage of the microgrid at critical area. First of all, the voltage outputs from VSO are evaluated and the bus with the maximum voltage violation is determined. Then, the PR searches for the nearest active DDG to this critical bus, using the Dijkstra algorithm. Then, the iterations go further with a predefined step size (based on hill climbing method). If the minimum point is exceeded the algorithm downsizes the steps for more accuracy and continues the iterations until the desired minimum point is achieved.

In each step of the hill climbing iteration, the new active power value (the old value plus the step size) of the DDG is sent to the CPLEX as a fixed (enforced) value. Then, the CPLEX conducts a new P-optimization for all other flexible units. In order to guarantee the convergence of the algorithm, the CPLEX is only allowed to change the UC & ED for all the time steps (hours) ahead and not the antecedent time steps. After the MILP calculation is performed, PFC and VSO update the Q-dispatching and power flow results considering the changed P-dispatching.

4.5. Unit recommitment (URC)

In some severe cases, especially in weak dimensioned microgrids, the previously mentioned optimization modules cannot solve the voltage problems totally, since the default unit commitment proposed by MILP is not appropriate for the problem. If any undervoltage violation remains after performing the PR-optimization, the URC will be activated, which leads to the test-wise variation of the UC and start-up of certain DDG(s). At first, the busses with the minimal voltages (after PR) are detected and then some nearest DDG (e.g. 3 DDG) are sorted using the Dijkstra algorithm, where the URC should be executed for them.

After enforcing a DDG in CPLEX to be online via URC, all optimization submodules should be refreshed. It means that the MILP conducts a new UC/ED (with considering the enforcement). Afterwards, the PFC examines the voltages under the new condition and if required, the next modules (VSO and then PR) will be activated. This process is repeated for all the DDG in the sorting list and finally the results of the different cases (different DDG) are evaluated.

4.6. RES curtailment (RESC) by overvoltages

If the enhancements resulted by the VSO and PR are not sufficient enough to meet the voltage limitations, the RESC module reduces the power injection of some RES units. The nearest RES to the violated bus is selected according to the Dijkstra method and then the curtailment occurs either in a continuous manner or stepwise based on the user predefined settings.

4.7. Current correction module for overloadings

In current correction a combination of the adjusted PR, URC and RESC has been utilized. Here PR finds two online DDG near both ends of the overloaded line, and redispatches the active power with hill climbing method, and evaluates the loading enhancement after each step. If one DDG is not enough, the next DDG can be redispatched. If the effect of already online DDG is not enough for solving the overvoltages, new DDGs will be activated by URC. In case of a huge integration of RES at the end of the branch, the PR cannot be effective anymore; thus, RESC reduces the active power injection of the units.

As can be seen, in contrast to GA, MILP-based optimizer starts from one solution point (the simplified linearized problem) and goes further with consideration of more different non-linear sub-problems (constraints) and solves them iterativly. In GA-based method, in each generation many solutions (number of population), which consider all possible constraints, are presented that leads to longer optimization time.

5. Analysis of EMS performance for a test microgrid

The tested radial LV (400 V line to line) microgrid with a MV/LV transformer (S_{rG} = 283 kVA) connected to upstream network via PCC is shown in Fig. 5.1. It has 22 busses, which are connected through 20 typical LV cables such as NA2XY 3x300sm with R/X ~ 1 (between 2–3, 3–12, and 2–17), NA2XY 3x150sm with R/X ~ 3 (between 12–14, 17–20, and 3–4), NFA2X 4x70sm with R/X ~ 5 (between 4–6, 12–15), and NA2XY 3x50sm with R/X ~ 9 (the rest of lines). The test system contains altogether 12 DER (6 PVs, 1 small wind turbine, 2 micro gas turbines, 1 fuel cell and 2 diesel gensets) and 1 battery storage system (200 kW/400 kW h). The total installed dispatchable power is approximately 425 kW, and the amount of non-dispatchable (only curtailable) RES power is 427 kW. 16 loads are distributed in the grid, which demand approximately 492 kW peak power and 8.2 MW h energy per day according to standard load profile (e.g. Germany H0) [49].

One of the decisive inputs for the microgrid dispatching is the energy exchange price. According to the data obtained from BDEW [50] dynamic import/export prices are defined for exchanged power with the interconnected grid. Fig. 5.2 illustrates the energy price profiles.

5.1. Microgrid operation in reference case study

Fig. 5.3 shows the cumulative overview of the P-dispatch of MG optimized with MILP in reference mode (REF). The red profile shows the sum of total loads and losses in the grid, which equals to the sum of all 9 generating units (considering main grid and BSS). The exchanged power profile between MG and main grid is not shown in this figure. The optimized BSS trend is clarified with black dotted profile. Since the operation of RES units is free of charge, their active power is always excluded from the EMS dispatching decided by MILP, as long as they do not violate system constraints, like maximum exchange power limit.

As expected before, due to low energy cost of FC, it is the most active DDG in this case study. In the peak load time and peak exchange price time (e.g. 8–10th h and 19–24th h), the FC works with full power and in other time intervals it operates at a working point, where it produces cheaper energy in comparison with main grid. The MT1 becomes online only in the time, when the demand is very high and the purchased energy cost may be higher than 27 € cent/kW h. It happens in the time interval of 20–23th hour in this case, where the MT1 works at its maximum efficiency point (200 kW). The BSS starts with SOC_{start} of 10% and is charged at 3–5th hour (lowest energy price) and discharged at 8th and 9th hours due to maximum import energy price. The same energy shifting process is occurred between 15–16th hour and 19–21th hour time intervals.

The optimal unit commitment (online and offline DDG in different time steps) obtained from GA as the best test between 10 tests is exactly the same as the MILP results, but due to randomness used in the GA process, minor differences can be found between dispatching of MILP and GA. Fig. 5.4 shows the operation cost trend

Please cite this article in press as: Nemati M et al. Optimization of unit commitment and economic dispatch in microgrids based on genetic algorithm and mixed integer linear programming. Appl Energy (2017), http://dx.doi.org/10.1016/j.apenergy.2017.07.007

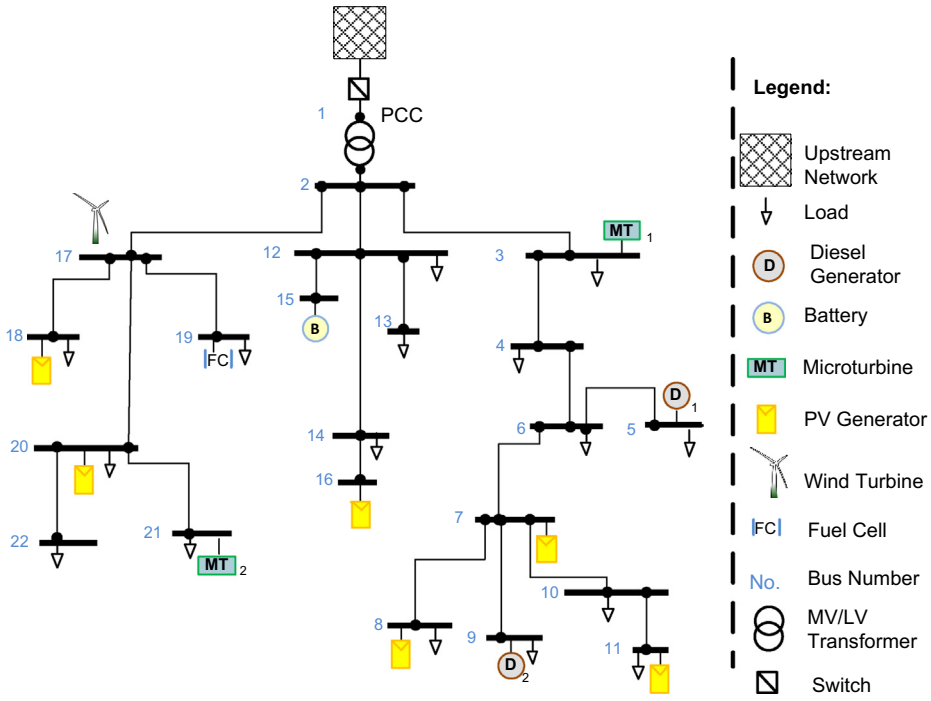

Fig. 5.1. Single phase Schema of the radial test LV microgrid.

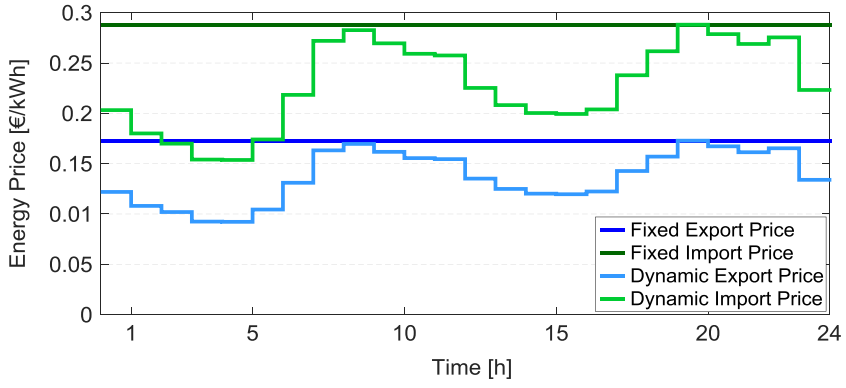

Fig. 5.2. Trend of dynamic and fixed exchange energy cost of microgrid and main grid.

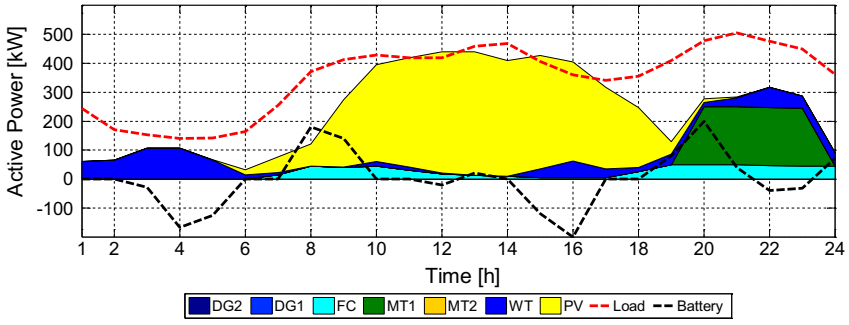

Fig. 5.3. Active power dispatch of microgrid components in reference mode optimized with MILP.

of 10 tests in GA in 200 generations that is compared with optimal operation cost found by MILP. The near optimal results of GA after 200 generations spread from 924 € to 930 €, which differ from MILP result (921 €) only 0.3%. The optimization time of the GA in this case is almost two times longer than MILP.

5.2. Sensitivity analysis of BSS aging in MOP1

Fig. 5.5 illustrates a sensitivity analysis of BSS dispatching conducted with GA under considering different aging levels in the objective function. Under "Aging level 1" (cost L1) the BSS has

Please cite this article in press as: Nemati M et al. Optimization of unit commitment and economic dispatch in microgrids based on genetic algorithm and mixed integer linear programming. Appl Energy (2017), http://dx.doi.org/10.1016/j.apenergy.2017.07.007

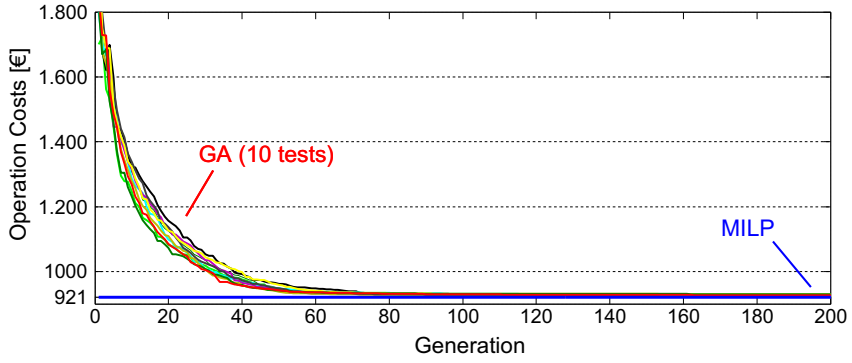

Fig. 5.4. Operation cost trend of MG optimized with GA in comparison with MILP result.

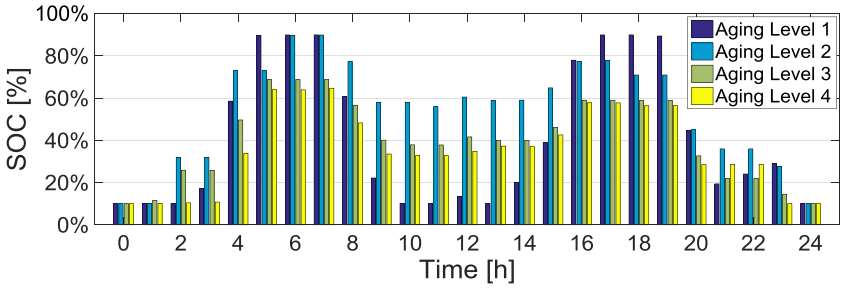

Fig. 5.5. SOC of BSS with different aging levels optimized with GA (sensitivity analysis of aging costs in objective function).

the maximum activity in order to shift the energy from low-cost periods to high-cost periods. This active BSS dispatch requires more than two full cycles (one cycle is 320 kW h). In "Aging level 2", (cost L2) the optimizer tries to find a compromise between load shifting and BSS aging minimization. It can be understood from the Fig. 5.5 that the length of microcycles is regulated and big microcycles, which can be seen in "Aging level 1", are prevented in this dispatching. With this dispatching strategy, the activity of the BSS is reduced to overall 414 kW h that equals 1.3 full cycles per day. In the case "Aging level 3" (cost L3), the extra impact of macrocycles is also considered. The overall energy exchange of BSS in this configuration is reduced further to 327 kW h (almost 1 full-cycle), which equals 53% activity reduction in a day ahead dispatching. In "Aging level 4" (cost L4) the microcycles, macrocycles and also SOC-factor are considered in $C_{BSS,t}$. As a result, beside reduction of partial cycles lengths, the average SOC in a day ahead dispatching of BSS is decreased to 37% (in REF: 42.7%).

Table 5.1 shows an overview of the important results under considering different BSS aging levels. In the table, total daily cost of the microgrid can be compared with daily aging cost of the BSS under consideration of different aging levels. Based on daily BSS aging, the whole life time of the BSS is calculated.

Fig. 5.6 shows the results of 50 (5 cases and 10 tests for each case) feasible tests of GA in 400 generations with different BSS considerations. The operational cost without utilization of any BSS is about 1005 € and comparable with total operational and aging costs in the reference case. In the other 3 cases, the total costs extend between 965 and 981 €.

It is assumed that the BSS is utilized only for day-ahead dispatching. With these assumptions and analyzing the Table 5.1 and Fig. 5.6, it can be recognized that the consideration of the BSS aging (from level 1 to level 4) can be a reasonable way to reduce the total cost defined in the objective function of MOP1 up to 4%. Moreover, the life time of the BSS can be extended to more than 25 years if it operates under considering the aging level 4.

5.3. Consideration of network constraints under MOP2

As analyzed in reference mode, some units like FC and the main grid act as the main suppliers to minimize the MG operation costs. With the resulted power flow, maximum voltage violations may occur at the end of the cables especially in the right branch, where no local DDG are online at the peak load periods. Furthermore, the overloading in this branch is very likely to happen. Under MOP2 the permitted voltage constraints are narrowed to 1.05 pu and 0.95 pu.

5.3.1. Analysis of GA performance with voltage and current constraints

The first noticeable point in MOP2 is the change in the unit commitment, so that the DG2 at the end of the right branch becomes online in order to keep the voltage limits of the branch.

Table 5.1
Overview of sensitivity analysis results for BSS aging costs optimized with GA.

Aging Level	MG Daily Operation cost [€]	BSS daily Aging cost [€]	BSS Life time [years]	Capacity usage (Cycles) [kW h]	Mean SOC
Aging-Level-1	924.48	82.03	4.00	691.75	0.427
Aging-Level-2	947.62	18.10	18.16	414.10	0.560
Aging-Level-3	957.9	15.75	20.87	326.86	0.415
Aging-Level-4	958.02	12.95	25.39	321.51	0.371

Please cite this article in press as: Nemati M et al. Optimization of unit commitment and economic dispatch in microgrids based on genetic algorithm and mixed integer linear programming. Appl Energy (2017), http://dx.doi.org/10.1016/j.apenergy.2017.07.007

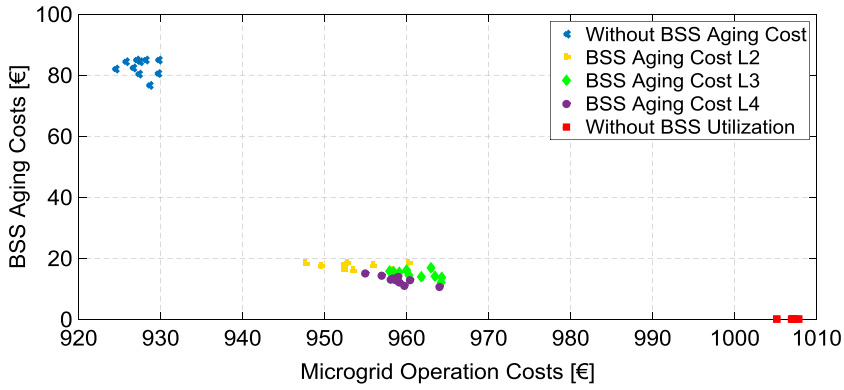

Fig. 5.6. Analysis of microgrid total daily operation costs vs. BSS daily aging costs with different aging levels (5 cases/10 GA-tests for each case).

On the other hand, the MT1 operates with maximum power to reduce the voltage drop through line 2–3. Since MT2 is far from the critical busses, it stays offline. The DG1 has a maximum power of 40 kW which is not enough for solving voltage violation in this area. The efficiency of DG2 in this power spectrum (30–40 kW) is better than DG1. Table 5.2 overviews the P/Q dispatching in critical hours. In this case, due to overloading problem in cables between node 2 and node 7, both diesel gensets are activated in some time steps to supply the loads locally, and the main grid and MT1 reduce their power outputs. In the 8th hour, only DG1 goes online (unit recommitment), because with 25 kW, the problem can be solved. The DG1 has a better efficiency in this operation point. Because of an overloading in line 17–20 in hour 21 the MT2 is activated.

With the dispatch manipulations in MOP2, the voltages are properly improved as illustrated in Fig. 5.7. The minimum voltages, which often are related to node 11, exceed the voltage limit between 19th hour and 24th hour in the reference mode.

5.4. Microgrid operation in islanded mode (MOP3)

In island mode, MILP utilizes often the fuel cell for the base load, while MT1 helps in the semi-peak load time and MT2 is activated

Table 5.2
P-Q-dispatch in MOP2 with consideration of voltage and current constraints in GA (green: unit recommitment, orange: considerable dispatch change, white: no change).

Hour [h]	8		19		20		21		22		23		24	
kW | kvar	P	Q	P	Q	P	Q	P	Q	P	Q	P	Q	P	Q
Main grid	59	-37	77	-86	2	-5	-1	-22	73	-31	17	-24	188	-65
DG1	25	-8	0	0	40	-13	40	-13	31	-10	36	-12	25	-8
DG2	0	0	50	-16	51	-16	65	-21	62	-20	43	-14	36	-12
FC	42	-8	38	+11	50	-15	50	-16	50	-16	50	-16	39	-13
MT1	0	0	159	-52	199	-66	135	-45	193	-57	200	-51	0	0
MT2	0	0	0	0	0	0	42	+6	0	0	0	0	0	0
BSS	168	-48	-1	0	108	-34	135	-44	-7	+2	55	-16	29	-10

Unit Recommitment Considerable dispatch change

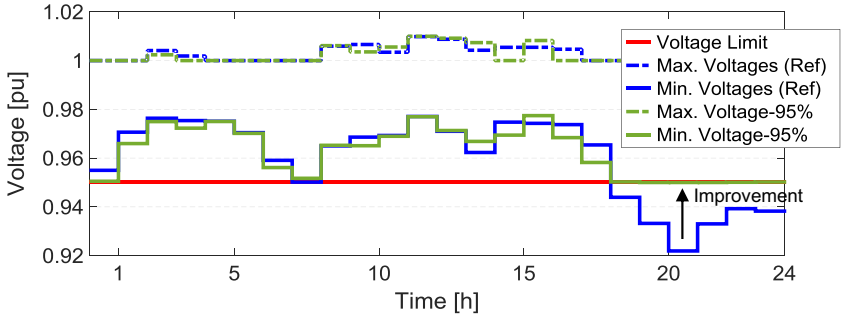

Fig. 5.7. GA results – Min and Max voltages in the grid in Ref mode vs. MOP2.

Please cite this article in press as: Nemati M et al. Optimization of unit commitment and economic dispatch in microgrids based on genetic algorithm and mixed integer linear programming. Appl Energy (2017), http://dx.doi.org/10.1016/j.apenergy.2017.07.007

in peak load time. In addition, the DG2 must be activated in time steps 20–23 in order to meet the demand in this period. In the islanded mode, the BSS, as a grid forming unit, must meet the energy balance between generation and demand. Fig. 5.8 shows the optimal P-dispatch of the microgrid in islanded mode.

5.5. Reduction of greenhouse gases production under MOP4

The objective functions of two modes are mixed considering a leveling and a weighting factor.

$$\text{Min}\{C_{Combined} = W_{Op} * C_{Op} + W_{Em} * R_{Op/Em} * C_{Em}\} \quad W_{Op} + W_{Em} = 1$$

where $C_{Combined}$ is the mixed operation and emission costs, C_{Op} is the operation cost, and C_{Em} is the emission cost. Also W_{Op} and W_{Em} represent weighting factors of each cost, and $R_{Op/Em}$ levels the order of the costs. By varying the weighting factors between 0 and 1, the combined optimal solutions known as pareto-optimal set can be achieved. Fig. 5.9 shows the resulted pareto front of MILP in comparison with pareto-optimal set of GA.

The results show the relatively dominance of MILP to GA optimization, especially in combined-objectives cases (e.g. weighting factors of $W_{Op} = 0.7$, $W_{Em} = 0.3$), while in the tests with quasi absolute objectives, the gap between MILP and GA is insignificant. It is basically because of leveling factor effect, which pushes the convergence of algorithm in direction of dominant objective function.

It is also interesting to observe the reduction trend of each emission type with descending W_{Op}. In Fig. 5.10 the trends of

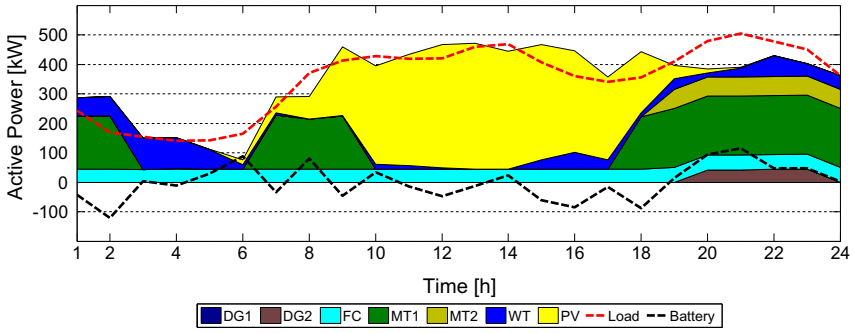

Fig. 5.8. P-dispatch of the microgrid in islanded mode (MOP3) optimized with MILP.

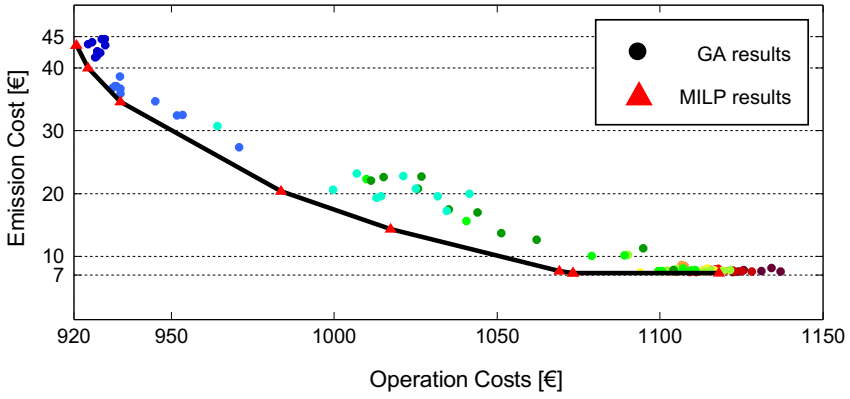

Fig. 5.9. Pareto-optimal set of operation and emission costs with different weighting factors – Considering only the microgrid operation – (Pareto front of MILP vs. pareto scatter diagram of GA).

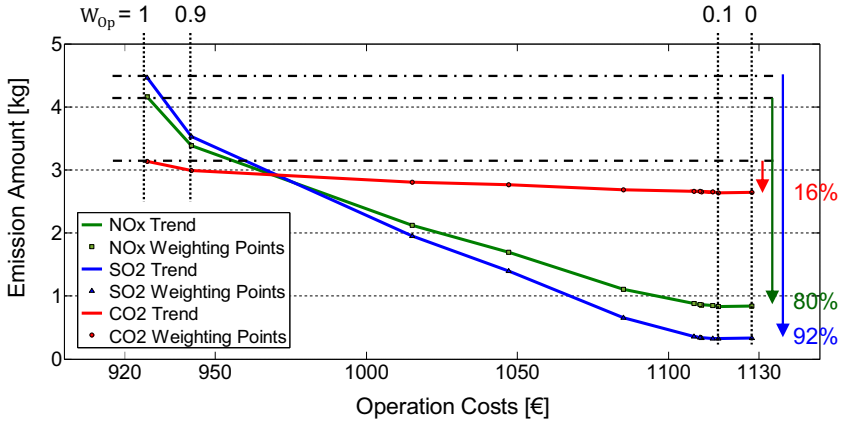

Fig. 5.10. Emission amount trend vs. operation cost trend in combined MOP4 mode regarding the weighting factors in GA.

Please cite this article in press as: Nemati M et al. Optimization of unit commitment and economic dispatch in microgrids based on genetic algorithm and mixed integer linear programming. Appl Energy (2017), http://dx.doi.org/10.1016/j.apenergy.2017.07.007

NO_x, SO_2, and CO_2 amounts dependent on the weighting factors are illustrated, which represent the best performance of GA between 10 tests with each weighting factor.

With varying W_{Op} from 1 to 0, the productions of SO_2, NO_x and CO_2 are reduced by almost 92%, 80% and 16% respectively. Because the CO_2 production rate of all units is in the same order (Table 2.2), the reduction of CO_2 emission is small.

5.6. Performance of GA in highly constrained multi-objective problem of MOP5

In this multi-objective operation mode, all aspects of last MOPs are considered with their priorities as explained in Section 2. The goal is to obtain a compromise between all quality aspects and to profit from different MG operation opportunities. The weightings of operation costs and emission costs are same here. In Fig. 5.11 the optimization processes of the operation cost, fitness rate and penalty rate have been depicted for the simulated MOP5 case. Due to a highly constrained problem, oscillations occur in the fitness rate of some generations, which are related to re-adjustment process of penalty weights.

The GA requires about 210 generations to solve all violations (mainly voltage, current and P-balance); Then the penalty weightings are re-adjusted in a manner that the optimizer searches the feasible region border because the optimal solutions are normally located in these areas. The average operation cost in this case equals 1194 € (an increase of 4.2% in comparison to results of MOP3). Also average emission cost has been increased by 45 € compared to results in MOP 4. Fig. 5.12 shows the minimum voltages and the maximum cable loadings (pu) in the microgrid (often in the right branch of the network). At the early and late peak load of the day the current limit has been reached but it is not exceeded. In addition, because of extra power injection (from DG1 and DG2) for branch 3–7 relief, the voltage has been shifted up (green curve).

Due to the activation of the DGs in 8 time steps, the operation and emission costs have been highly raised. But in comparison to MOP2, where no emission is considered at all, the maximum value of emission costs shows a reduction of 13%. The averaged value of BSS aging costs (Level 4) is almost doubled compared to average result of MOP1, while the minimum value of BSS life time (5.9 years) indicates an improvement of 34% in comparison to reference mode (3.9 years). Table 5.3 shows an overview of different costs.

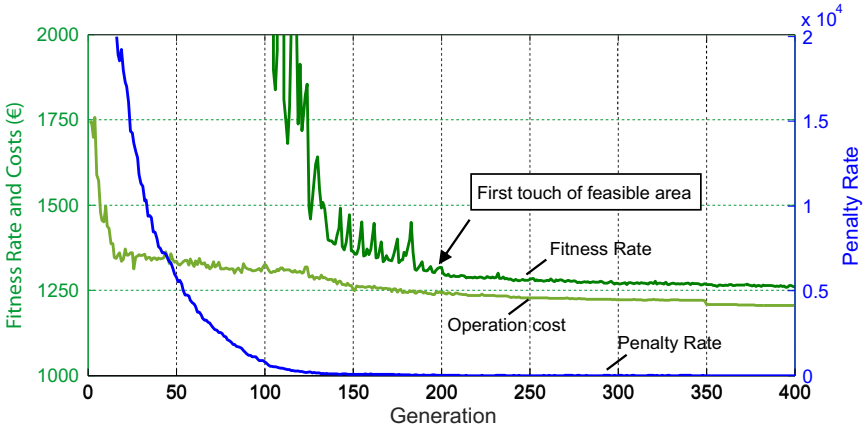

Fig. 5.11. Trends of cost, fitness and penalty rate in 400 generations under MOP5.

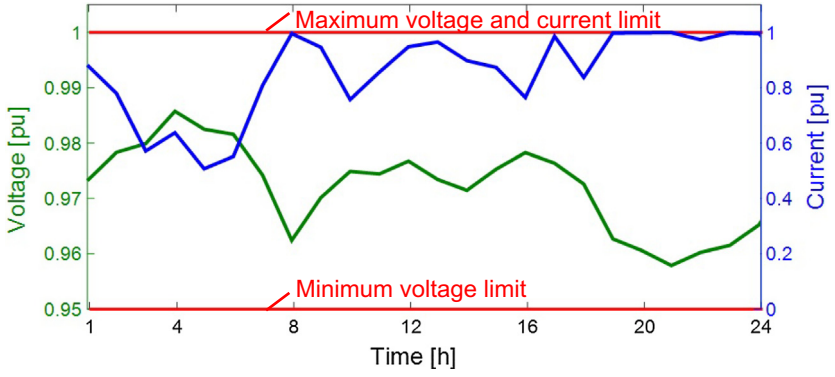

Fig. 5.12. Minimum voltage and maximum loading in the MG under P-Q-dispatch of MOP5.

Table 5.3
Overview of different system costs under MOP5 in comparison with other MOPs.

	Average (MOP5)	Minimum (MOP5)	Maximum (MOP5)	Average in related MOP	Best-Worst in Other MOPs
Operation Costs [€]	1194	1177	1215	1146 (MOP3)	924–1161
Emission Costs [€]	53	44	70	8 (MOP4)	7–79
BSS Aging Cost [€]	31.2	19.3	55.7	16.1 (MOP1)	13–85
BSS Life Time [Year]	10.5	5.9	17	20.4 (MOP1)	25.4–3.9

Please cite this article in press as: Nemati M et al. Optimization of unit commitment and economic dispatch in microgrids based on genetic algorithm and mixed integer linear programming. Appl Energy (2017), http://dx.doi.org/10.1016/j.apenergy.2017.07.007

6. Conclusions

This paper presents two algorithms, which are applied to the universal microgrid EMS for performing an optimal day-ahead unit commitment and an economic dispatch. The developed EMS contains a spectrum of new components, different operation policies and two different optimizers of UC/ED to guaranty and validate the quality of results. A new Li-Ion battery aging model based on an event-driven aging behavior has been developed, which considers the impacts of partial cycles and SOC-rate on the BSS life time. Different optimization objective functions and constraints under different microgrid operation policies such as cost-efficient, grid supporting, maximum islanding degree, eco-friendly, and multi-functional operations are pre-defined in EMS.

As the first UC and ED optimizer, a new GA-based optimization mechanism based on different flexible and case-specific sub-operators has been developed. With the new developed priority-based initialization method in GA, minimum constraint violation can happen at the beginning of the generations, which shift the solutions near to the border of feasible area. About 40% enhancement in the feasibility of the end results can be seen in comparison to the random initialization method in this case. Also a new adoptable method, namely DTX, for recombination of individuals was developed for the GA concept, which profits from the searching ability of SBX and fast convergence of SPX and TPX methods. Moreover, due to inability of usual random mutation method, two new mutation concepts, namely SPM and ASPM, which can prevent violations (e.g. min up/down time) in mutation process, are developed. Different penalty weighting factor adjustment methods are used in the fitness function, which can adjust the weighting factors in different manners over the generations. The adjustments are dependent on the development of the constraints violations of the fittest individual. The adoptive continuous penalty method seems to be more robust and fast for finding the global optimum region in high-constrained problems.

As the second optimizer, a novel method is introduced to deal with the limitations of the MILP algorithm for handling the network topology constraints via decomposition of the mixed integer non-linear problem into a MILP-based economic dispatch problem and a non-linear OPF problem. Different sub-modules such as voltage setpoint optimizer for a smart reactive power adjustment, P-Redispatcher for iterative active power dispatch correction, unit recommitment via manipulations in CPLEX, RES curtailment unit and current correction module are integrated in the non-linear optimizer. The main benefits of this method in comparison to classical OPF are full consideration of network constraints, no simplification in power flow calculation, smart manipulations in CPLEX results and selective activation of different optimizer modules.

In the cases without consideration of the network constraints like REF, MOP3 and MOP4, the calculation time of the GA is comparable with the MILP, but in MOP2, the MILP needs 84% shorter time to converge than the GA. In all cases except MOP2 and MOP5 the MILP shows always slightly better results than GA. In high constrained cases such as MOP2 and MOP5, the GA shows relatively better results in comparison to MILP. The voltage and loading violations are remedied very precisely via GA, while due to the recursive and iterative P/Q optimization process in MILP, less accuracy in voltage and loading improvement can be seen in some cases.

Under maximum constraints level (MOP5), the GA takes about 210 generations to solve all violations (in reference case almost 10 generations). In this case 22% increase of the operation cost in comparison to reference case has been resulted.

With consideration of the BSS full economic model, the BSS (cycle life) aging costs and the total microgrid costs (MOP1) have been reduced up to 84% and 4%, respectively.

In future works some further improvements could be done. Under highly constrained cases (e.g. MOP2) the manipulation of the DDGs' P-dispatching in CPLEX and the iterative extern P/Q corrections, causes a fine mismatch and shifting of working point of the DGs from optimal points. To solve this problem, either the whole calculations must be linearized and done via CPLEX or the whole concept should be replaced with a MIQP (Quadratic MINLP) concept.

Furthermore, one improvement that can be made to the GA presented in this paper is to involve more GA parameters in the searching process, in order to get a more/fully self-adoptive system. One idea is to divide the population into some groups (islands) and use the results of high-ranked islands for other islands in next generations.

References

[1] Fang X, Misra S, Xue G, Yang D. Smart grid—the new and improved power grid: a survey. IEEE Commun Surv Tutorials 2012;14(4):944–80.
[2] Soshinskaya M, Crijns-Graus WH, Guerrero JM, Vasquez JC. Microgrids: experiences, barriers and success factors. Renew Sustain Energy Rev 2014;40:659–72.
[3] Braun M, Strauss P. A review on aggregation approaches of controllable distributed energy units in electrical power systems. Int J Distrib Energy Resources 2008;4:297–319.
[4] Liang H, Zhuang W. Stochastic modeling and optimization in a microgrid: a survey. Energies 2014;7(4):2027–50.
[5] Soares A, Antunes CH, Oliveira C, Gomes Á. A multi-objective genetic approach to domestic load scheduling in an energy management system. Energy 2014;77:144–52.
[6] Amini MH et al. Distributed security constrained economic dispatch. In: 2015 IEEE Innovative Smart Grid Technologies-Asia (ISGT ASIA). IEEE; 2015.
[7] El-Sehiemy RA, El-Hosseini MA, Hassanien AE. Multiobjective real-coded genetic algorithm for economic/environmental dispatch problem. Stud Inform Control 2013;22(2):113–22.
[8] Rigo-Mariani R, Sareni B, Roboam X, Turpin C. Optimal power dispatching strategies in smart-microgrids with storage". Renew Sustain Energy Rev 2014;40:649–58.
[9] Jin Xiaolong et al. Dynamic economic dispatch of a hybrid energy microgrid considering building based virtual energy storage system. Appl Energy 2016.
[10] Boroojeni KG et al. An economic dispatch algorithm for congestion management of smart power networks. Energy Syst 2016:1–25.
[11] Logenthiran Thillainathan, et al. Multi-Agent System (MAS) for short-term generation scheduling of a microgrid. In: IEEE International Conference Sustainable Energy Technologies (ICSET); 2010.
[12] Farhat IA. Economic and economic-emission operation of all-thermal and hydro-thermal power generation systems using bacterial foraging optimization (Doctoral dissertation). Dalhousie University Halifax; 2012.
[13] Zhang Jingrui et al. A hybrid harmony search algorithm with differential evolution for day-ahead scheduling problem of a microgrid with consideration of power flow constraints. Appl Energy 2016;183:791–804.
[14] Wang Luhao et al. Integrated scheduling of energy supply and demand in microgrids under uncertainty: a robust multi-objective optimization approach. Energy 2017.
[15] Lee KY, El-Sharkawi MA., Editors. Modern heuristic optimization techniques: theory and applications to power systems. vol. 39. John Wiley & Sons; 2008.
[16] Li B, Roche R, Miraoui A. Microgrid sizing with combined evolutionary algorithm and MILP unit commitment. Appl Energy 2017;188:547–62.
[17] Parisio A, Rikos E, Glielmo L. A model predictive control approach to microgrid operation optimization. IEEE Trans Control Syst Technol 2014;22(5):1813–27.
[18] Olivares DE, Cañizares CA, Kazerani MA. centralized optimal energy management system for microgrids. IEEE Power Energy Soc General Meeting 2011(1–6).
[19] Wu X, Wang X, Bie Z. Optimal generation scheduling of a microgrid. In: 2012 3rd IEEE PES Innovative Smart Grid Technologies Europe (ISGT Europe) (1–7); 2012.
[20] Lasnier F, Ang TG. Photovoltaic engineering handbook. Adam Hilger, New York: IOP Publishing Ltd; 1990.
[21] Quaschning V. Regenerative energiesysteme: technologie-berechnung-simulation. Carl Hanser Verlag GmbH Co KG 2015.
[22] Deshmukh MK, Deshmukh SS. Modeling of hybrid renewable energy systems. Renew Sustain Energy Rev 2008;12(1):235–49.
[23] Chedid R, Akiki H, Rahman S. A decision support technique for the design of hybrid solar–wind power systems. IEEE Trans Energy Convers 1998;13(1):76–83.
[24] Zhu J. Optimization of power system operation. John Wiley & Sons; 2015.
[25] Faisal M. Microgrid modelling and online management; 2008.
[26] Walters CD, Sheble BG. Genetic algorithm solution of economic dispatch with valve point loading. IEEE Trans Power Syst 1993;8(3):1325–32.

Please cite this article in press as: Nemati M et al. Optimization of unit commitment and economic dispatch in microgrids based on genetic algorithm and mixed integer linear programming. Appl Energy (2017), http://dx.doi.org/10.1016/j.apenergy.2017.07.007

[27] Staffell I. A review of small stationary fuel cell performance. University of Birmingham; 2009.
[28] Kabza A. Fuel Cell Formulary; 2013.
[29] Li X. Understanding the design and performance of distributed tri-generation systems for home and neighborhood refueling. University of California, DavisInstitute of Transportation Studies; 2012.
[30] Mohamed Faisal A, Koivo Heikki N. System modelling and online optimal management of microgrid using mesh adaptive direct search. Int J Electric Power Energy Syst 2010;32(5):398–407.
[31] Campanari S, Macchi E. Technical and tariff scenarios effect on microturbine trigenerative applications. J Eng Gas Turb Power 2004;126:581–9.
[32] Farret FA, Simões MG. Integration of alternative sources of energy. IEEE press; 2006.
[33] Pipattanasomporn M, Willingham M, Rahman S. Implications of on-site distributed generation for commercial/industrial facilities. IEEE Trans Power Syst 2005;20(1):206–12.
[34] Weston F, Seidman NL, James C. Model Regulations for the output of specified air emissions from smaller-scale Electric Generation Resources.. Regul Assist Project 2001.
[35] Gerschler JB. Ortsaufgelöste Modellbildung von Lithium-Ionen-Systemen unter spezieller Berücksichtigung der Batteriealterung, Aachen: Shaker, ISBN 978-3-8440-1307-8; 2012.
[36] Küpper M. Flexibles Batteriemanagementsystem für Lithium-Ionen-Traktionsbatterien in Hybrid- und Elektrofahrzeuganwendungen. Aachen: RWTH Aachen; 2012.
[37] Su W, Wang J. Energy management systems in microgrid operations. Electricity J 2012;25(8):45–60.
[38] Badey Q, Cherouvrier G, Reynier Y, Duffault J-M, Franger S. Ageing forecast of lithium-Ion batteries for electric and hybrid vehicles. Curr Top Electrochem 2011;16:65–79.
[39] Sauer DU, Wenzl H. Comparison of different approaches for lifetime prediction of electrochemical systems—using lead-acid batteries as example. J Power Sources 2008;176(2):534–46.
[40] Indradip M, Degner T, Braun M. Distributed generation and microgrids for small island electrification in developing countries: a review. Sol Energy Soc India 2008;18(1):6–20.
[41] Technical Brochure 635, "Microgrids", first report of WG C6.22; 2015.
[42] Nemati M, Bennimar K, Tao L, Müller H, Braun M, Tenbohlen S. Optimization of microgrids short term operation based on an enhanced genetic algorithm. In: IEEE PES Powertech conference, Eindhoven; 2015.
[43] Nemati M, Zöller T, Tao L, Müller H, Braun M, Tenbohlen S. Optimal energy management system for future microgrids with tight operating constraints. Lisbon: IEEE PESEuropean Energy Market; 2015.
[44] Nemati M, Eberlein S, Tao L, Müller H, Braun M, Tenbohlen S. Optimale Einsatzplanung dezentraler Anlagen in Mikrostromnetzen mittels genetischem Algorithmus. Smart Cities, Frankfurt: VDE Kongress; 2014.
[45] Senjyu T, Shimabukuro K, Uezato K, Funabashi T. A fast technique for unit commitment problem by extended priority list. IEEE Trans Power Syst 2003;18(2):882–8.
[46] Deb K, Agrawal RB. Simulated binary crossover for continuous search space. Complex Syst 1994;9(3):1–15.
[47] Li Y, Pedroni N, Zio E. A memetic evolutionary multi-objective optimization method for environmental power unit commitment. IEEE Transac-tions Power Systems 2013:2660–9.
[48] Liu W, Zhang Y, Zeng B, Niu S, Zhang J, Xiao Y. An environmental-economic dispatch method for smart microgrids using VSS_QGA. J Appl Math 2014.
[49] Standardlastprofile, BDEW Bundesverband der Energie- und Wasserwirtschaft e.V; 2015.
[50] Strompreisanalyse, BDEW Bundesverband der Energie- und Wasserwirtschaft e.V; 2015.

Please cite this article in press as: Nemati M et al. Optimization of unit commitment and economic dispatch in microgrids based on genetic algorithm and mixed integer linear programming. Appl Energy (2017), http://dx.doi.org/10.1016/j.apenergy.2017.07.007